Universidade de Aveiro
2017

Departamento de Ciências Médicas

Marisa de Almeida Pereira

Identification of human tRNA modifying enzymes involved in protein aggregation

Identificação de enzimas modificadoras de tRNA humano envolvidas na agregação proteica

Universidade de Aveiro
2017

Departamento de Ciências Médicas

Marisa de Almeida Pereira

Identification of human tRNA modifying enzymes involved in protein aggregation

Identificação de enzimas modificadoras de tRNA humano envolvidas na agregação proteica

Dissertação apresentada à Universidade de Aveiro para cumprimento dos requisitos necessários à obtenção do grau de Mestre em Biomedicina Molecular, realizada sob a orientação científica da Doutora Ana Raquel Santos Calhôa Mano Soares, Investigadora de pós-doutoramento do Departamento de Ciências Médicas da Universidade de Aveiro.

Apoio financeiro pela Fundação Portuguesa de Ciência e Tecnologia através do POCI-COMPETE2020, FEDER, UID/BIM/04501/2013 e PTDC/BIM-MEC/1719/2014.

FCT Fundação para a Ciência e a Tecnologia
MINISTÉRIO DA CIÊNCIA, TECNOLOGIA E ENSINO SUPERIOR
COMPETE 2020
PROGRAMA OPERACIONAL COMPETITIVIDADE E INTERNACIONALIZAÇÃO
PORTUGAL 2020
UNIÃO EUROPEIA
Fundos Europeus Estruturais e de Investimento

“Cada pessoa deve trabalhar para o seu aperfeiçoamento e, ao mesmo tempo, participar da responsabilidade coletiva por toda a humanidade.”

Marie Curie, Novel Prize in Physics and Chemistry, 1903 /1911.

presidente	Doutora Ana Gabriela da Silva Cavaleiro Henriques Professora auxiliar do Departamento de Ciências Médicas da Universidade de Aveiro
arguente	Doutora Denisa Daud Mateus Investigadora de pós-doutoramento na Unidade de Genómica do Biocant – Associação de Transferência de Tecnologia
orientador científico	Doutora Ana Raquel Santos Calhôa Mano Soares Investigadora de pós-doutoramento do Departamento de Ciências Médicas da Universidade de Aveiro

agradecimentos

Primeiramente, e acima de tudo eu gostaria de agradecer à minha orientadora, Ana Soares e a uma grande amiga, Sandra Carmo, pela forma como me guiaram através de inúmeras dificuldades, pelo entusiasmo, sugestões e esforços que foram indispensáveis. Gostaria ainda, de aproveitar esta oportunidade para agradecer à turma de Mestrado em Biomedicina Molecular do ano letivo 2015/2016 e aos parceiros de laboratório cujas contribuições foram essenciais na concretização do presente projeto científico. Finalmente, um agradecimento muito especial à minha irmã, Ana Sofia Pereira – por despertar o melhor de mim – pais e avós, pelo seu apoio constante, ajuda inestimável e estímulo contínuo.

"A gratidão é a memória do coração."

Antístenes

palavras-chave RNA de transferência; síntese proteica; erros de tradução; siRNA; *stress* proteotóxico; enzimas modificadoras de tRNA; agregação proteica; vias de controlo de qualidade.

resumo

As doenças conformacionais são caracterizadas pela acumulação de agregados proteicos, destabilização da síntese de proteínas e *stress* proteotóxico devido a mutações, *desregulação* da rede de *stress* e defeitos na maquinaria de tradução. No entanto, os mecanismos subjacentes a estes fenótipos ainda não são totalmente compreendidos. Os tRNAs são moléculas essenciais para a tradução e são extensamente modificados. Estas modificações são essenciais para a estabilidade do tRNA e para o correto emparelhamento codão-anticodão e são catalisadas por diferentes classes de enzimas modificadoras de tRNA. Recentemente, algumas dessas enzimas, em particular as que catalisam modificações na região do anticodão do tRNA foram encontradas desreguladas em várias doenças, nomeadamente cancro, distúrbios metabólicos e neurológicos.

A ligação entre as enzimas modificadoras de tRNA e o *stress* proteotóxico como mecanismo subjacente da doença não se encontra experimentalmente demonstrada. Assim, estabelecemos a hipótese de que a desregulação destas enzimas - especialmente aquelas que catalisam modificações na posição 34 - afetam a fidelidade da tradução, resultando na agregação de proteínas e na ativação da UPR, características das doenças acima mencionadas.

Para testar esta hipótese, implementámos um método fluorescente baseado em siRNAs em células HeLa expressando um sistema repórter de agregação desenvolvido por nós. Das enzimas testadas, o silenciamento das que pertencem ao *Elongator Acetyltransferase Complex* (ELP) levou à acumulação mais marcante de focos fluorescentes nas células, indicando a ocorrência de agregação de proteínas. Experiências adicionais demonstraram que a taxa de síntese proteica é afetada, bem como a morfologia mitocondrial e alguns mecanismos de controlo de qualidade.

Este estudo preliminar demonstra pela primeira vez, em células de mamífero que existe uma ligação entre as enzimas modificadoras de tRNA e a acumulação de agregados proteicos, indicando que estas moléculas podem ser importantes alvos terapêuticos nas doenças conformacionais.

keywords Transfer RNA; protein synthesis; translation errors; siRNA; proteotoxic stress; tRNA modifying enzymes; protein aggregation; protein quality control.

abstract

Protein conformational diseases are characterized by accumulation of protein aggregates, impaired protein synthesis and proteotoxic stress due to mutations, down regulation of the stress network and defects in the translation machinery. However, the mechanisms underlying these phenotypes are not yet understood. tRNAs are main players of the translation machinery and tRNA modifications are essential for efficient codon-anticodon recognition influencing translation efficiency. These modifications are catalyzed by different classes of tRNA modifying enzymes that have been found deregulated in several diseases, namely cancer, metabolic and neurological disorders.

The connection between tRNA modifying enzymes and proteotoxic stress as an underlying mechanism of disease was not experimentally demonstrated. We have hypothesized that deregulation of these enzymes – especially those that catalyze modifications at position 34 – affect translation fidelity, resulting in protein aggregation and UPR activation, hallmarks of the above-mentioned diseases.

To test this hypothesis, we implemented a tRNA modifying enzyme fluorescent based siRNA screen in HeLa cells expressing a protein aggregation reporter system developed by us. From all the tested enzymes, knockdown of the ones belonging to the Elongator Acetyltransferase Complex (ELP) family led to the most striking accumulation of fluorescent *foci* in cells, indicating that protein aggregation was occurring. Additional experiments demonstrated that protein synthesis, mitochondrial morphology and some quality control mechanisms were also affected.

This preliminary study demonstrates for the first time in mammalian cells a relation between tRNA modifying enzymes deregulation and accumulation of protein aggregates, indicating that these enzymes can constitute relevant novel therapeutic targets in conformational diseases.

DECLARAÇÃO

Declaro que este trabalho é integralmente da minha autoria, estando devidamente referenciadas as fontes e obras consultadas, bem como identificadas, de modo claro, as citações dessas obras. Não contém, por isso, qualquer tipo de plágio, quer de textos publicados, quer de trabalhos académicos, qualquer que seja o meio dessa publicação, incluindo meios eletrónicos.

Assinatura: _____ Data: ___/___/____

Contents

I. List of abbreviations

AA-AMP	Aminoacyl Adenylate
ADAT3	Adenosine Deaminase, tRNA - specific 3
ALKBH8	Methyltransferase Alkylation repair homolog 8
ARD	Aging Related Diseases
ARS	Aminoacyl-tRNA synthetase
ASL	Anticodon Stem-Loop
ATF4	Activating Transcription Factor 4
ATF6	Activating Transcription Factor 6
ATP	Adenosine Triphosphate
BCA	Bovine Serum Albumin
BiP	Binding immunoglobulin Protein
bZIP	basic Leucine zipper
C	Cytidine
CMA	Chaperone-mediated autophagy
CNS	Central nervous system
DMEM	Dulbecco's Modified Eagle Medium
DUBs	Deubiquitinating enzymes
eIF	Translation eukaryotic initiation factor
ELB	Empigen Lysis Buffer
ELP3	Elongator protein 3 homolog
ER	Endoplasmic reticulum
ERAD	ER-associated degradation
eRF	Eukaryotic release
ERSE	ER stress-response element factor
FBS	Fetal Bovine Serum
FTSJ1	RNA Methyltransferase Homolog1
G	Guanosine
GAPDH	Glyceraldedyde 3-phosphate dehydrogenase
GTP	Guanosine triphosphate
HD	Huntington Disease
HSP	Heat Shock Protein
IRE1	Inositol-requiring enzyme 1
IRS-1	Insulin receptor substrate-1
MERRF	Myoclonus epilepsy ragged-red fibers
METTL1	Methyltransferase like 1

mRNA	mature messenger RNA
MS	Multiple Sclerosis
MTU1	Mitochondrial tRNA-specific 2- thiouridylase
NRF2	Erythroid 2-related factor 2
NSUN2	NOP2/Sun RNA methyltransferase family member 2
PABP	Poly-A binding protein
PBS	Phosphate Buffered Saline
PCR	Polymerase Chain Reaction
PD	Parkinson Disease
PERK	PKR-like ER kinase or Pancreatic Endoplasmic Reticulum-resident Kinase
PFA	Paraformaldehyde solution
PN	Proteostasis Network
Ppi	Pyrophosphate molecule
QCM	Quality control mechanisms
RIDD	Regulated Ire1-dependent decay
RISC	RNA Induced Silencing Complex
RNA	Ribonucleic Acid
RP	Regulatory particle
RT	Room Temperature
ROS	Reactive Oxygen Species
SDS-PAGE	Sodium Dodecyl Sulfate-Polyacrylamide Gel Electrophoresis
siRNA	small interfere RNA
SOD1	Superoxide dismutase 1
TAE	Tris-Acetato-EDTA buffer
TBS-T	Tris-saline buffer with tween 20
TiMES	tRNA Modifying Enzymes Screening
TRAF2	TNFR-associated factor 2
tRFs	tRNA fragments
tRNA	transfer RNA
U	Uridine
UPP	Ubiquitin-proteasome pathway
UPR	Unfolded protein response
VMP1	Vacuole membrane protein 1

II. List of figures

III. List of tables

CHAPTER 1.

Introduction

1.1 From RNA to protein

The determination of the iconic three-dimensional structure of the DNA double helix by Watson and Crick reversed the understanding of life. This discovery led Crick to formulate the central dogma of genetic information that includes how DNA replication occurs, its transcription into ribonucleic acid (RNA) and translation into protein (1,2).

The instructions to build proteins are encoded in the cells' DNA. As described in the central dogma of molecular biology, information from a gene can be used to build a protein in a two-steps process. The first – **transcription** – in which the DNA sequence of a gene acts as a template for synthesis of an RNA transcript. In eukaryotes, this transcript goes through additional processing steps to become a mature messenger RNA (mRNA). In the second – **translation** – the nucleotide sequence of the mature messenger RNA (mRNA) is "decoded" to build a polypeptide product (a protein or protein subunit) with a specific sequence of amino acids (3).

In an mRNA, the sequences of three nucleotides (codons) are used to build a polypeptide. There are 61 different codons that code for 20-22 amino acids. This means that some amino acids are encoded by multiple codons and this is why the genetic code is **degenerate**. Three additional *stop-codons*, UAA, UAG, and UGA, indicate when a polypeptide is completely formed. One codon, AUG, specifies the amino acid methionine and works as a *start-signal*, simultaneously (4).

This group of codon-amino acid relationships is called the **genetic code**, as it allows a nucleotide sequence to be *decoded* into a chain of amino acids. This code is nearly **universal**. With only minor exceptions, a single coding dictionary is used by almost all viruses, prokaryotes, archaea, and eukaryotes, as shown in figure 1. The deciphering of the genetic code and the demonstration of its universality represented one of the most important discoveries in biology (5).

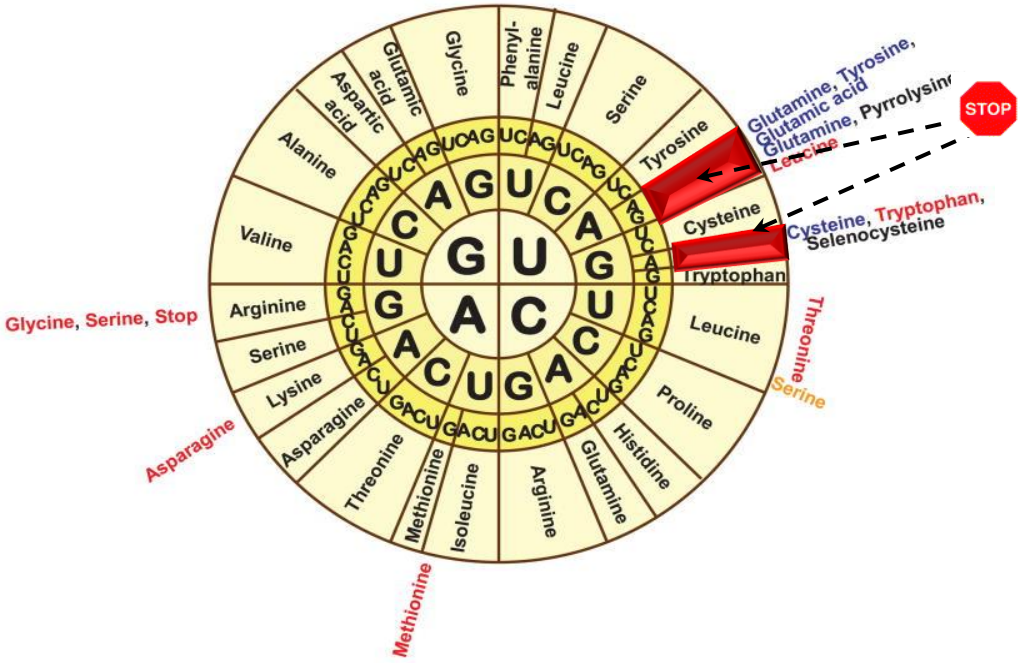

Figure 1: Representation of the genetic code and its variations: the amino acids are specified by each mRNA codon (constituted by three nucleotides). Multiple codons can code for the same amino acid. Differences to the standard genetic code are shown in red for mitochondrial, blue for ciliate and Euplotid nuclear code, and orange for the ambiguous yeast nuclear code. Sec and Pyl are shown in black. Adapted from: (6).

During translation, the codons of an mRNA transcript are read sequentially (from 5' to 3') by special RNA molecules called tRNAs. Each of them recognizes just one or a few codons and delivers the corresponding amino acid, which is added to the C-terminus (carboxyl group end) of the growing polypeptide. In this way, a chain of amino acids is built, one at a time and the sequence of amino acids in the chain reflects the sequence of codons found in the mRNA. Once a *stop-codon* is reached, the polypeptide is complete (6).

The acuity in information transference is carefully controlled at each step during gene expression. The most *error-prone* steps occur at the ribosome, where an aminoacyltRNA is matched with the corresponding codon on the messenger RNA, and an amino acid is paired with a tRNA by an enzyme, aminoacyl-tRNA synthetase (ARS). With a few exceptions, *errors* from the aminoacylation reaction cannot be fixed, which almost – with an error rate as shown in the figure 2 – inevitably leads to the incorporation of the wrong amino acid during protein synthesis (7).

As a consequence, the cells activate mechanisms capable to tolerate certain degree of errors. However, if there are other factors that lead to an increase of these errors, the cells are probably not able to get rid of the wrong proteins and this can lead to proteotoxic stress – where catastrophic loss of accuracy in protein synthesis can occur (8).

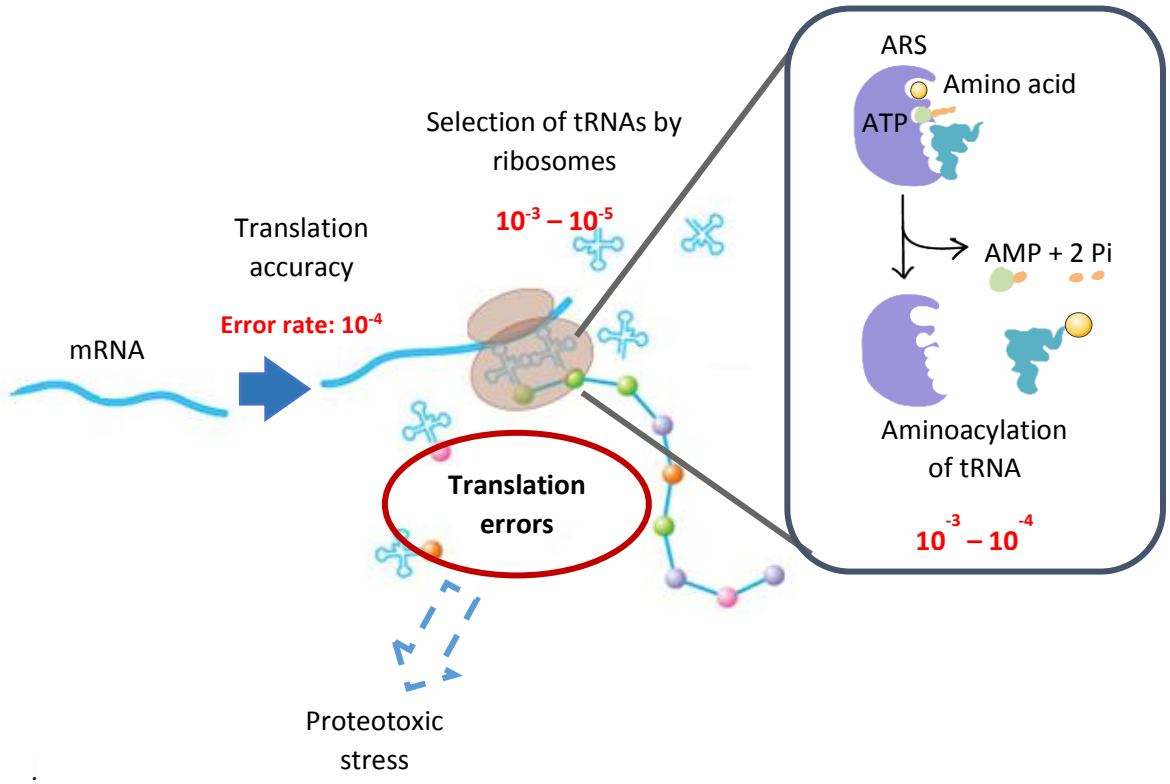

Figure 2: Translation enables the transfer of information from the messenger RNA into an amino-acid sequence at ribosomes, thanks to the amino-acid-specific transfer RNAs (tRNAs). Both steps of this process are prone to error (typical rates are shown in red). The inset shows the aminoacylation of tRNA, in which an amino acid is paired with a tRNA by the corresponding ARS. Once synthesized, a protein usually becomes functional. In some cases, however, misfolding occurs. Most misfolded proteins are degraded by the cell – but if the degree of misfolding surpasses the cell capacity to deal with those proteins, some can form insoluble aggregates that, can lead to states of proteotoxic stress that are characteristic of conformational disorders, for example neurological diseases. Adapted from: (7).

1.1.1 The three stages of the process

The translation process, as a dynamic and continuous process, can be subdivided into three major stages: initiation; elongation; and termination of the polypeptide chain and its recycling (9).

Stage 1: Initiation

The first step in translation is the assembly of the initiation complex, which consists of an mRNA, the small (40S) and large (60S) ribosomal subunits, and an initiator tRNA, carrying one amino acid in the P-site – specified by the first codon, or *start-codon*, of an mRNA coding sequence. When completely assembled, the initiation complex consists of a ribosome *sandwiched* around an mRNA, with the initiator tRNA bounded to a *start-codon*. A group of proteins called eukaryotic initiation factors (eIFs) (Table 1) help to assemble the initiation complex using energy provided by hydrolysis of adenosine triphosphate (ATP) or guanosine triphosphate (GTP), an energy storage molecule similar to ATP (10,11).

Initiation factors eIF1A, eIF3 bind to the 40S ribosomal subunit. The initiator tRNA bearing methionine is bounded by eIF2 (complexed with the GTP), and form a complex with the 40S subunit and eIF1. The 5' cap of an mRNA is attached to this ribosomal subunit by eIF4E, eIF4G – which binds to both eIF4E at the 5´ cap and poly-A binding protein (PABP) at the 3´poly-A tail - eIF4A, and eIF4B. Then, the ribosome goes downstream in the 3' direction until it reaches the *start-codon*, AUG. This process is known as scanning, and the small subunit may scan through hundreds of nucleotides before reaching the *start-codon*, requiring energy obtained by ATP hydrolysis. Once a *start-codon* has been selected, eIF5 triggers the hydrolysis of guanosine triphosphate (GTP) bounded to eIF2 – complex to GDP – and other initiation factors. The 60S ribosomal subunit joins the 40S complex, enabled by eIF5B and establishes the initial conditions for translation (7).

Stage 2: Elongation

Elongation occurs when the polypeptide chain gets longer, with the addition of new amino acids. In elongation, the ribosome moves along the mRNA in the 5’ to 3’ direction. The ribosome has three sites for tRNA binding, namely the P (peptidyl), A (aminoacyl), and E (exit) sites. The initiator methionyl-tRNA binds to the P site and the next aminoacyl-tRNA binds to the A site, by pairing with the second codon of the mRNA (7).

The aminoacyl-tRNAs are chaperoned to the ribosome by elongation factors (eEF1α) enabling amino acids incorporation, one-by-one, to the C-*terminus* (carboxyl group end). A linear chain of amino acids (polypeptide) with the N and C *termini* are marked. The N-*terminus* has an exposed amino group. The C-*terminus* has an exposed carboxyl group. The carboxyl group

exposed at the C-*terminus* of a polypeptide reacts with the amino group of an incoming amino acid, forming a peptide bond. This reaction adds the new amino acid to the chain. The carboxyl group of the newly added amino acid becomes the new C-*terminus* of the polypeptide (12).

During translocation, the ribosome moves one codon over on the mRNA towards the 3' end. This shifts the tRNA from the A to the P site and the tRNA from the P to the E site. The empty tRNA in the E site leaves the ribosome. When the entire coding sequence of the mRNA has been read, a *stop-codon* will get into the A site of the ribosome, signalling that the polypeptide is completely formed and must be released (13).

Stage 3: Termination and recycling

Termination is the stage in which translation ends and the completed polypeptide is released. It occurs when a *stop-codon* (UAG, UAA, or UGA) gets into the A site of the ribosome and a protein called a release factor (eRF1) binds to it. The binding of the release factor causes a water molecule to be added to the end of the polypeptide (in place of an amino acid), breaking the bond that connects it to the tRNA in the P site, resulting in a release of the completed polypeptide from the ribosome (9). Finally, the ribosome-recycling occurs, which is characterized by the release of ribosomes from the mRNA after termination and splitting of the ribosome (10).

Table 1: Some factors and functions associated with the translation process. Adapted from:(9).

Factor	Known Function in Translation
eIF1	AUG recognition
eIF1A (IF1)	Scanning/ AUG recognition
eIF2 (IF2)	Met-tRNA binding
eIF2B	Recycles eIF2 (guanine nucleotide exchange factor)
eIF3 (IF3)	Ribosome binding
eIF4A	RNA Helicase
eIF4B	Facilitates eIF4A activity
eIF4E	Cap-binding
eIF4F	Complex of eIF4E, 4G and 4A
eIF4G	Scaffold protein
eIF5	GAP (GTPase-activator protein)
eIF5B (IF2)	Late stage in initiation, promotes subunit joining
PABP	Binds poly (A) and eIF4G

1.2 Transfer RNAs

In 1957, Francis Crick[1] proposed the existence of an "*adaptor molecule*" that could covalently bind to the amino acid and also be capable of hydrogen bonding to a nucleotide sequence (13). Now, we know that the Crick's prediction was correct – the transfer RNA (tRNA) – serves as the adaptor in protein synthesis, and the ribosome accommodates two tRNA molecules at a time, as previously described (14).

The first nucleic acid to be completely sequenced was the tRNA that binds the amino acid alanine ($tRNA^{Ala}$) from yeast. Of great interest was the finding that a number of nucleotides are unique to tRNA, each containing a so-called *modified base.* This pioneering work was performed by Holley and co-workers long before the invention of today's rapid sequencing techniques. For his work, Holley received the 1968 Nobel Prize in Physiology or Medicine (15).

Holley's sequence analysis led him to propose the two-dimensional cloverleaf model of the tRNA molecule. It had been known that tRNA molecules have a characteristic secondary structure created by base pairing. He discovered that the linear sequence could be arranged in such a way that several stretches of base pairing would be formed. His arrangement, with its series of paired stems and unpaired loops, resembled the shape of a three-clover leaf. The loops consistently contained modified bases that did not generally form base pairs (16).

There are 4 arms and 3 loops: the loop closest to the 5' end is called the dihydrouridine arm (D arm) because it contains dihydrouridine bases, which are unusual nucleotides common only to tRNA. The loop closest to the 3' end is called the T arm, after its sequence of thymine-pseudouridine-cytosine (pseudouridine is also an unusual base). The loop on the bottom of the cloverleaf contains the anticodon, which binds complementarily to the mRNA codon. Because anticodons bind with codons in the antiparallel method, they are written from the 5' end to 3' end, the inverse of codons (Figure 3). The genetic code relies on the interaction between the three bases of the mRNA's codon triplet (numbered 1, 2, and 3) and the three anticodon bases of the cognate aminoacyl-tRNA (numbered 36, 35, and 34 in the anticodon stem loop) (17).

[1] In **1955** Crick wrote **"On Degenerate Templates and the Adaptor Hypothesis"**, an unpublished paper which predicts the existence of transfer ribonucleic acid (tRNA); In **1957**, proposes the **"Sequence Hypothesis"** and the "**Central Dogma**," path-breaking concepts about how genetic information is encoded in DNA and controls protein synthesis. <*In National Library of Medicine (NLM)>. https://profiles.nlm.nih.gov/ps/display/About at 22 of July of 2016.*

Although the standard rules of the Watson-Crick pairing (A/U, U/A, G/C, C/G) strictly govern the interaction between base pairs 1/36 and 2/35, the 3/34 base pairing can be nonstandard (wobble interaction) (17).

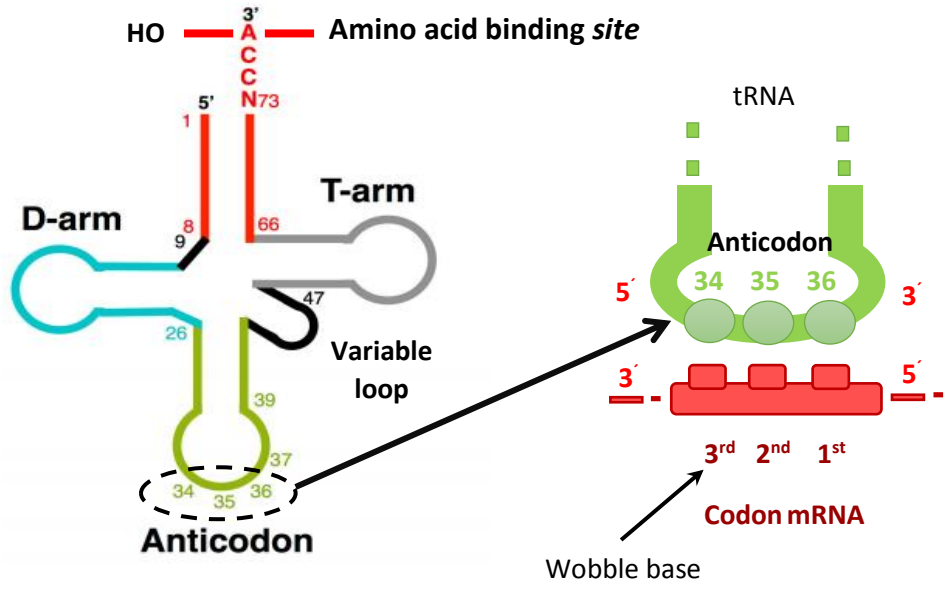

Figure 3: Illustration of Holley's two-dimensional model of transfer RNA. Different organisms use distinct but convergent strategies to optimize decoding by modifying specific tRNAs, predominantly at position 34 of the Anticodon Stem-Loop (ASL) (which interacts with the third codon base via non-Watson-Crick base pairing or wobble base pairing). Adapted from: (110, 111).

Posterior studies on this molecule have allowed the identification of 30 – 40 different tRNA in bacterial cells and around 50 - 100 tRNAs in animals and plant cells. The number of tRNAs in most cells is larger than the number of amino acids found in proteins – 20-22 – and also differs from the number of codons in the genetic code. Consequently, many amino acids have more than one tRNA to which they can attach; in addition, many tRNAs can attach to more than one codon. As noted previously, most amino acids are encoded by more than one codon, requiring some tRNAs to recognize more than one codon (17).

Immediately after synthesis, the tRNA, like all RNAs, contains the four bases A, G, C and U. However, mature tRNAs can contain modified bases – different from the canonical bases mentioned above. These modifications are introduced after transcription of the tRNA and the most modified bases occur at restricted sites. The first base in the anticodon, the wobble position, often contains modified bases that allow the formation of unusual base pairs with the third base in the mRNA codon (18).

Subsequently, maturation of the tRNAs is required, which happens *via* several steps through pre-RNAs or primary tRNAs. In the first step, the transcription of tRNA genes in pre-tRNA is accomplished by the activity of an enzyme termed RNA polymerase III. Next, the sequences – 5' leader and 3' trailer of the pre-tRNA structure – are removed from endonucleolytic cleavage catalyzed by RNase P and RNase Z, correspondingly. Next the trinucleotides "CCA" are attached to the 3' *termini* of tRNAs through CCA-adding enzymes. It is noteworthy that modification events occur at this stage, resulting in different non-canonical bases at various positions. Lastly, the resulting mature tRNA is aminoacylated by their aminoacyl-tRNA synthetases cognates, and participate in the translation process at the ribosome (Figure 4) (19,20). Both – pre-mature tRNA and mature tRNA – serve as substrates for the production of tRNA fragments (TRFs) a novel class of regulatory non-small RNAs that are beyond the scope of this thesis (20).

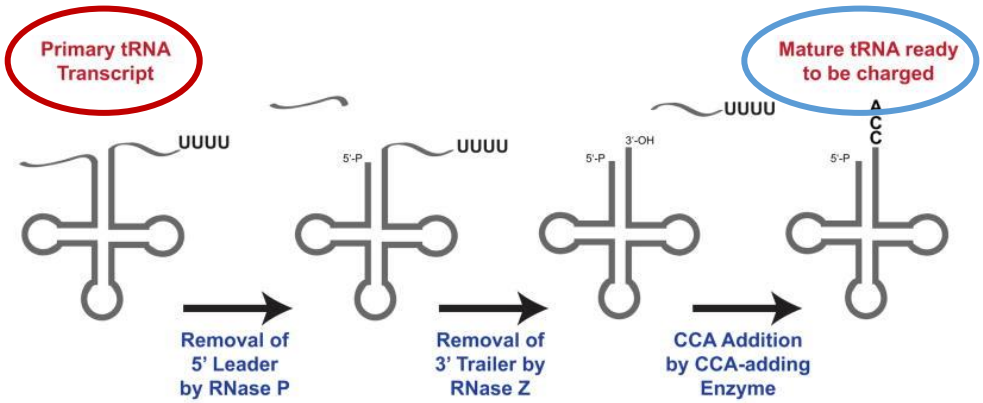

Figure 4: Process of maturation of tRNAs: Once transcribed, tRNAs are sequentially processed at their 5' and 3' ends to generate a mature tRNA that can be charged with an amino acid. The 5' leader sequence is almost universally cleaved off by the endonuclease RNase P, while multiple mechanisms have been reported for tRNA 3' end processing. In humans, the endonuclease RNase Z cleaves downstream of the unpaired discriminator base, releasing the 3' trailer sequence. Finally, the addition of specific enzymes of nucleotide "CCA" at the 3' terminal of tRNA occurs. Adapted from: (19).

In this process of decoding the genetic message, the recognition of the codon or codons specifying a given amino acid by a particular tRNA is actually the second step. The first step is the attachment of the appropriate amino acid to a tRNA, catalyzed by a specific ARS. In 1957, Paul Zamecnick and Mahlon Hoagland discovered this group of 20 enzymes (one for each amino acid), and they have been related to diseases such as cancer, neuronal disorders, autoimmune disorders, among others (21,22).

In detail, each ARS charges a specific tRNA molecule with its cognate amino acid *via a* two-step enzymatic reaction. In the first step, the ARS binds the amino acid and ATP molecule to form the aminoacyl adenylate (AA-AMP) intermediate, and a pyrophosphate molecule (Ppi) is released. In the second step, a tRNA molecule binds the ARS *via* the anticodon binding domain, and the amino acid is transferred to the tRNA. An AMP molecule is then released, followed by the charged tRNA and the ARS is free to charge another tRNA molecule (23).

1.2.1 tRNA modifications

Post-transcriptional modification is a critical processing step – catalyzed by tRNA modifying enzymes – that results in functional tRNA molecules, allowing folding, stability and decoding (24). Over the years, modified nucleosides have been sequenced, and the type and location of each one has been identified in GtRNAdb, MODOMICS and RNApathwaysDB databases. Different tRNAs are able to suffer different modifications at specific positions. It reflects the evolutionary conservation among tRNAs from the three domains of life. Also, complex modifications require several enzymes (25). In general, hypomodified tRNAs are targeted for degradation since they can have negative consequences for cells, such as reduce protein production, to ribosome pausing at cognate codons. These results suggest that the chemical complexity is necessary to maintain the homeostasis of translational process (26).

1.2.2 Types and functions of tRNA modifications

Modified nucleotides are generally characterized by relatively simple chemical structures, such as: the addition of one (or sometimes two) methyl groups to various positions of the nucleotide bases and or ribose sugars, replacement of oxygen with sulfur (in s_2U), isomerization or reduction of the uridine base to pseudouridine or dihydrouridine, respectively, or addition of other relatively small chemical functional groups (i.e., acetylation and threonylation) (27). More specifically, wobble modifications, at the position 34, include uridine (U) modifications through incorporation of hydroxyl, methyl, and thiol groups and adenosine (A) modifications such as adenosine-to-inosine (A-to-I) editing (28). Adding cm^5U group on uridines at the wobble position requires the six-subunit Elongator (ELP) complex. That, in association with methyltransferase Alkylation repair homolog 8 (ALKBH8), catalyzes the formation of 5-methoxycarbonyl-methyluridine (mcm^5U) at the wobble position. This substrate can be thiolate

by an enzymatic cascade involving Urm1, Uba4, Ctu1, Ncs2 and Ncs6 to yield mcm^5s^2U (Figure 5) (28).

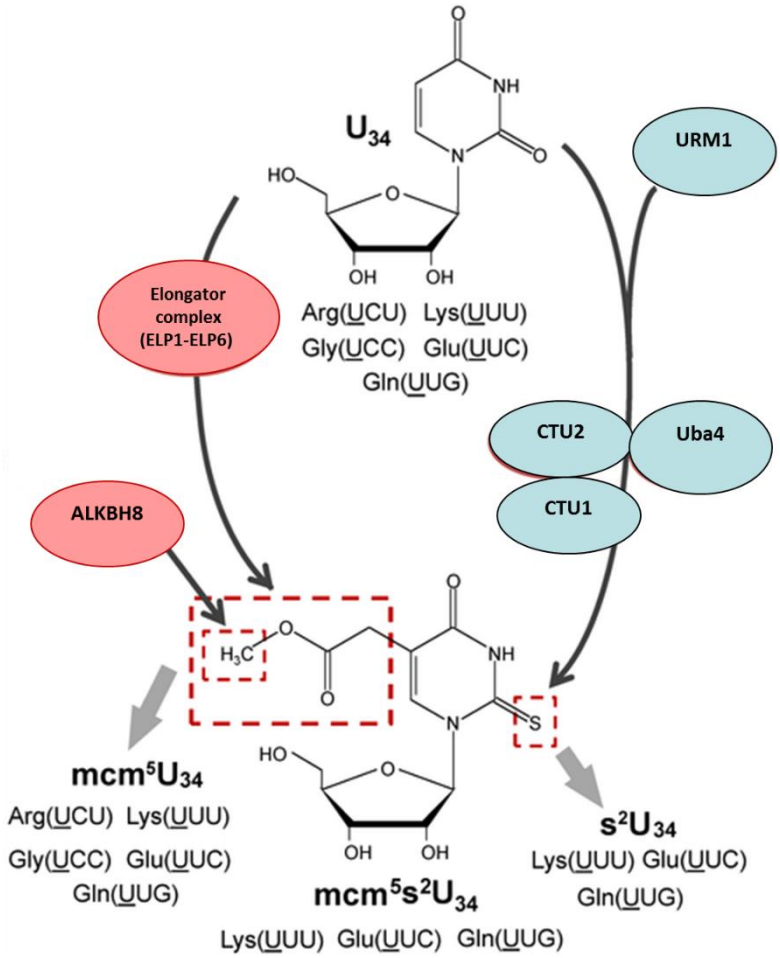

Figure 5: Chemical modifications associated the enzymes of Elongator Complex, ALKBH8 and others. Adapted from: (28).

Modifications in the stem–loops are crucial for tRNA structure and stability. The pseudouridines modifications can act in sugar conformation of the nucleobases, increasing binding affinity and rigidify the tRNA structure; on the other hand, dihydrouridines modifications help to maintain the flexibility of the tRNA structure (26). However, modifications in the anticodon loop can directly affect the tRNA function in translation and increase the accuracy by reading frame maintenance or preventing translational frameshifting (29). Modifications at position 34 are generally associated with decoding by increasing the diversity of codon recognition through codon–anticodon wobbling. Modification at this site is conserved in bacteria and eukaryotes, which has evolved in parallel to the species. Furthermore, post-transcriptional modifications at base 37, adjacent to the anticodon loop, help to stabilize codon–anticodon interactions by providing base-stacking interactions (16).

1.2.3 tRNA modifying enzymes and associated diseases

Several studies – in yeast and human homologs – have demonstrated the role played by these enzymes in tRNAs and some of those molecules have been associated with diseases (Figure 6) (Annexes Table 9):

The **adenosine deaminase, tRNA - specific 3** (**ADAT3**) catalyzes the deamination reaction of adenosines converting them in inosine at the position 34, 37 and 57 of tRNAs (30). A single missense mutation in humans (valine128-to-methionine substitution), that results in a loss of protein function, was recently reported in individuals affected with intellectual disabilities **–** from mild to profound – and strabismus (31).

The **RNA Methyltransferase Homolog 1** (**FTSJ1**) – encodes the methyltransferase required for mC_{32} and mG_{34} modification of $tRNA^{Phen}$ (32); mutations, such as substitution of Guanine655-to-Adenine and deletion of a guanine nucleotide in exon 2, are associated with different phenotypes, namely: Mental retardation X-linked type 44 (MRX44), Mental retardation, X-linked 99 and X-linked non-syndromic intellectual disability (32–34).

Also, allelic variants of **Elongator protein 3 homolog** (**ELP3)** have been associated with amyotrophic lateral sclerosis (ALS), and their knockdown in zebrafish resulted in motor axonal abnormalities (35). Also, the human ELP4 gene has been associated with Rolandic epilepsy, the most common type of human epilepsy (36).

The tRNA modifying enzymes, **NOP2/Sun RNA methyltransferase family member 2** (**NSUN2)** and **methyltransferase like 1** (**METTL1)** are mammalian orthologous of yeast Trm4 and Trm8, which are required for protecting tRNA against rapid tRNA decay. NSUN2 has been initially identified as a substrate of AURKB protein kinase in HeLa cells and encodes a methyltransferase that catalyzes the methylation of cytosine to 5-methylcytosine (m^5C) at position 34 of intron-containing $tRNA^{Leu}$ (CAA) precursors (37). This also happens at position 48, 49, and 50 in the variable arm of $tRNA^{Gly}$ (GCC) precursor (38). The mentioned modification is necessary to stabilize the anticodon-codon pairing and to the accuracy of the mRNA translation. In cases of mutations, mental retardation, autosomal recessive 5 (39) and Dubowitz syndrome are associated (38).

The METTL1 catalyzes the formation of N(7)-methylguanine at position 46 (m^7G^{46}) and has been initially identified as a substrate of PKBα – Akt/protein kinase Bα – in HeLa cells (40). In this case, a single nucleotide polymorphism (SNP) is associated and located at the 3' untranslated region (3' UTR) of the METTL1 gene and has been implicated in Multiple Sclerosis (MS) (41). **Mitochondrial tRNA-specific 2- thiouridylase 1** (**MTU1)** is a mitochondrial homolog

of bacterial MnmA. Its partial inactivation in cultured cells by siRNAs was shown to result in both a lack of s^2U formation and reduced mitochondrial oxygen consumption.

Mutated MTU1, acting as a modifier factor, modulates the phenotypic manifestation of the deafness-associated with 12S ribosomal RNA mutations (42). Moreover, mutations from cells of patients with myoclonus epilepsy associated with ragged-red fibers (MERRF), lacks the τm^5s^2 U modification (43). Figure 6 contains information collected from various studies that associate defects in tRNA modifications and human diseases such as cancer, T2D, neurological disorders, and mitochondrial-linked disorders (44).

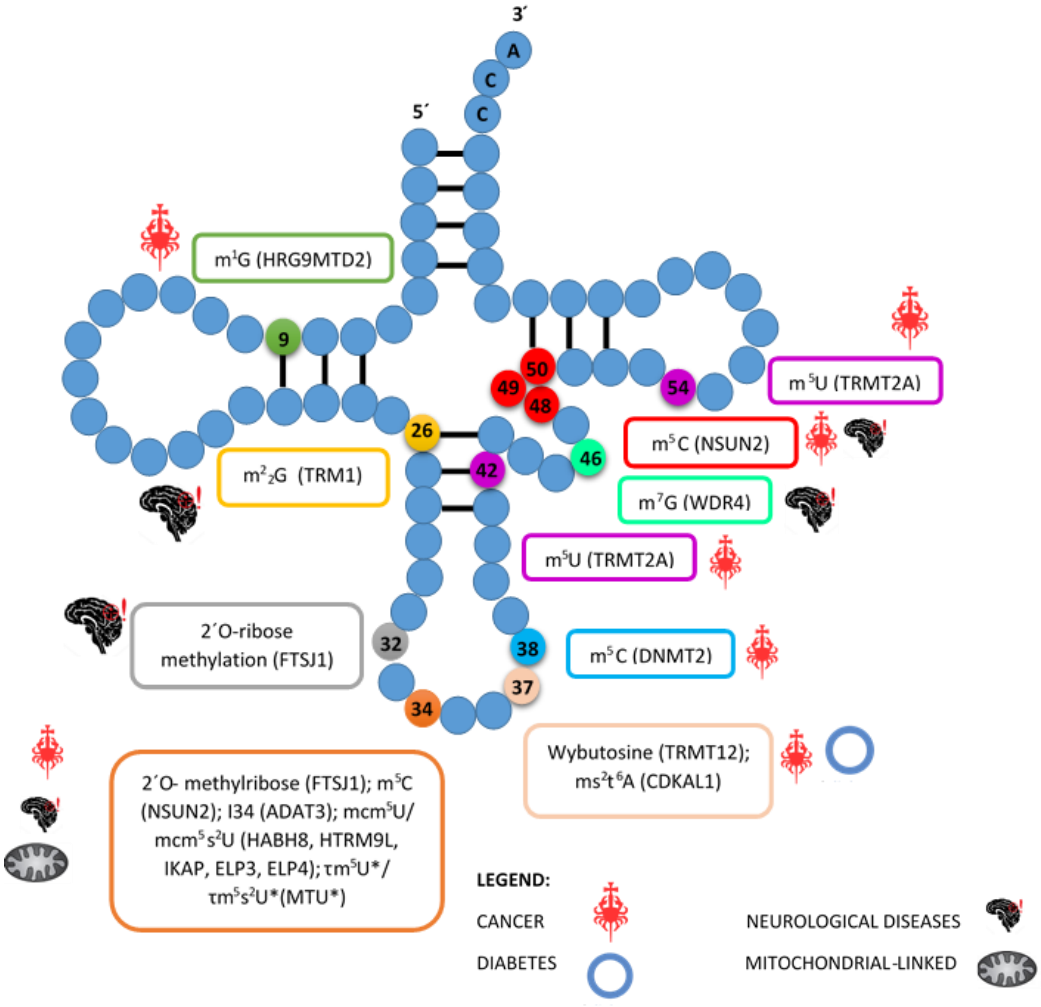

Figure 6: Schematic representation of the clover leaf tRNA secondary structure with respective modifications and tRNA modifying enzymes (in parenthesis) that catalyze them and that have been linked to human pathologies – illustration indicated in front of each box. Connecting lines between RNA residues indicate base pairing. Asterisks indicate modifications that are only found in mitochondrial tRNAs. Adapted from: (44).

1.2.4 Protein folding and misfolding

Once a polypeptide has been translated, it has to fold into the correct three-dimensional shape in order to work correctly. Some polypeptides must also be chemically modified, cleaved into smaller pieces, combined with other polypeptides, or shipped to particular organelles (45).

Proteins all begin their synthesis in the cytosol. Many of them are there permanently, but some are transported to other cellular destinations and some are completely synthesized in the cytosol. These may be imported into the mitochondrion, peroxisome, chloroplast, and nucleus *via* post-translational transport. Other proteins are co-translationally imported into the endoplasmic reticulum. From there, most go to the Golgi apparatus by vesicle transport to the cell exterior (for secretion), the plasma membrane, the lysosome, or other parts of the endomembrane system (46).

Most of the signalling proteins used by eukaryotic cells to communicate with their environment are assembled in the ER. This transmission and management of information through proteins are essential for sustaining cell function (47).

When proteins are correctly folded and they achieve their native conformation, the hydrophobic regions of the polypeptide are confined within the structure in order to maintain the lowest possible energy state (48).However, protein misfolding can occur due to mutations or environmental factors, that may contribute to expose the hydrophobic domains, promoting oligomerization and aggregation of the protein (49). During this process of aggregation, the exposed hydrophobic areas interact with other proteins, leading to malfunction of diverse cellular pathways (50). Quality control mechanisms (QCM) are activated, attempting to neutralize the damaging agent. Molecular chaperones, such as HSP70-family proteins, bind to hydrophobic polypeptide structure, blocking their interaction and minimizing aggregation (49).

The cell also attempts to target the aggregates to degradation, *via* the proteasomes or autophagy. If these attempts fail, as a last resource, the misfolded protein molecules assemble through beta sheet-containing domains into amyloid fibrils with cross-beta cores (51), which accumulate into large depositories where the hydrophobic areas are less exposed to damaging interactions. To sum up, the proteins have three major folding fates inside the cells in order to maintain proteostasis (Figure 7) (45).

Protein aggregation is a hallmark of conformational disorders, namely neurological diseases including Alzheimer's, Parkinson's or ALS. Despite the fact that in most of these diseases the misfolded protein is located in the cytosol or nucleus, paradoxically one main consequence is interference with processes in the endoplasmic reticulum (ER), causing ER stress and, in long-term, mitochondrial damage and cell death (52).

Indeed, there is an increasing evidence that this is the main pathway of cytotoxicity (53). In a recent study (54) it is referred that the aggregation in the cytoplasm interfered with a nucleus-cytoplasmic protein and RNA dislocation. In contrast, the same proteins did not inhibit location when forming inclusions in the nucleus and at/or around the nucleolus. Protein aggregation in the cytoplasm, but not in the nucleus, cause the appropriation and dislocation of proteins containing disordered and low complexity sequences. Impairment of nucleus-cytoplasmic dislocation may contribute to the cellular pathology of various aggregate deposition diseases (49).

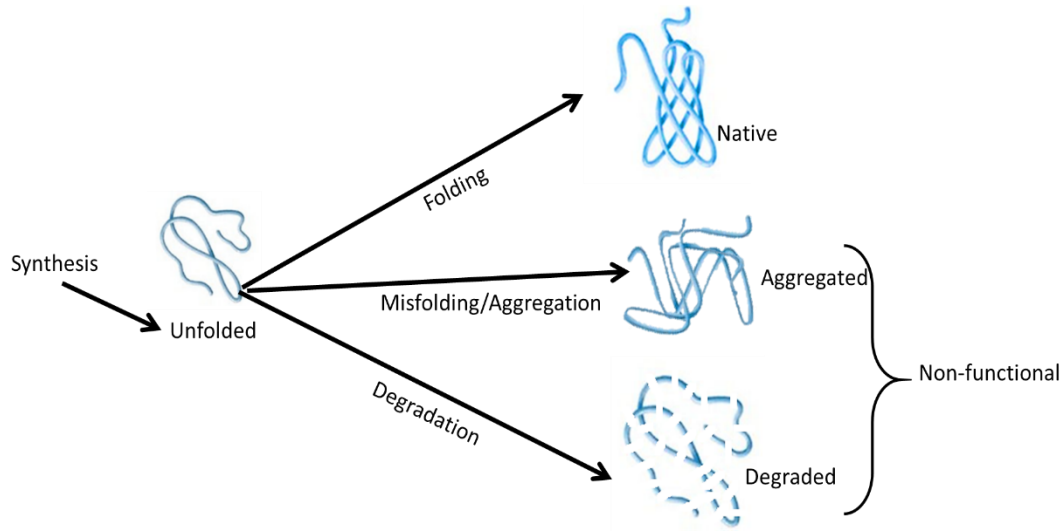

Figure 7: Protein fates in the Proteostasis Network (PN). The PN integrates chaperone pathways for the folding of newly synthesized proteins, the remodeling of misfolded states, and disaggregation with protein degradation.

1.3 Proteotoxic stress and protein quality control pathways:

Any error in protein folding for physiological or pathological processes may lead to ER stress and activates a set of signalling pathways described below (55) (48). The activation of these ER transmembrane receptors induces a series of transcription factors that targets an ER stress–response element (ERSE) in the promoter region of genes encoding for ER chaperone proteins, folding enzymes, and components of the ER-associated degradation (ERAD) process. The activation of these genes enhances the cell's folding capacity and the degradation of misfolded and aggregated proteins, allowing the cell to relieve the stress and restore ER homeostasis (56)(57) (Figure 25- Annexes).

1.3.1 Chaperones and heat shock response

Molecular chaperones are defined as an ubiquitous family of folding modulators that play a central role in the conformational quality control of the proteome by assisting and stabilizing the correct non-covalent assembly of polypeptides (58).

The chaperone function is associated with stabilization of unfolded proteins, translocation across membranes or degradation, and/or to assist in their correct folding and assembly. The large diverse family of molecular chaperones includes (but is not limited to) many heat-shock protein families. It is important to note that some heat-shock proteins are in the cell at a certain level all the time, even under non-stressed conditions. The heat-shock protein families include hsp40, hsp60, hsp70, hsp90, hsp100, and the "small hsps" (59). The numbers in the names of these families refer to the size of the corresponding protein, allowing the differentiation among them. For example, hsp70 has approximately 70,000 Daltons, a standard unit of measuring mass in proteins (37).

As a part of chaperone family, heat-shock proteins are essential, and the expression of some of them drastically increase during the heat-shock response (Table 2). These proteins can protect the cell by helping it to survive under conditions that would normally be lethal (59). Aggregates resulted for example, from neurodegenerative disease associated-proteins often take molecular chaperones, impairing proteostasis (60) (61).

Table 2: Families of molecular chaperones. Adapted from: (62).

Small heat shock proteins (HSP25)	Protect from cellular stress; prevent aggregation in the lens (cataract).
Small heat shock proteins (HSP27)	Inhibition of apoptosis; protection against oxidative stress and assist in protein degradation by the proteasome.
Hsp60 system (cpn60,GroEL) *ATPase*	Protein folding; prevention of aggregation.
Hsp70 system (DnaK, BiP) ATPase	Stabilization of extended chains; membrane translocation; unfolding; regulation of the heat shock response; targeting substrates for degradation.
Hsp90 *ATPase*	Binding, stabilization and maturation of steroid receptors and protein kinases; delivery to proteases; buffer for genetic variation; regulation of substrate selection and fate; myosin assembly.
Hsp100 (Clp) *ATPase*	Thermotolerance; proteolysis; resolubilization of aggregates; remodelling; unfolding.

1.3.2 Unfolded Protein Response (UPR)

Several studies state that mutations, environmental factors or ageing, may promote oligomerization and aggregation of proteins. Each of these situations can activate the UPR response *via* three ER transmembrane receptors: a) PKR-like ER kinase (PERK); b) Inositol-requiring enzyme 1 (IRE1); c) activating transcription factor 6 (ATF6) (63) (64) (Figure 9).

a) The Pancreatic Endoplasmic Reticulum-resident Kinase (PERK) Pathway

PERK (also called PKR-related ER-resident kinase) is a serine/threonine kinase and is a member of the eIF2 Kinase family. After activation, PERK's phosphorylates are the eukaryotic initiation factors, resulting in translation attenuation of transcripts with a 5´cap. This eIF2α phosphorylation reduces the protein load on the ER membranes and attenuates cell growth and proliferation. PERK has also been shown to be directly involved in phosphorylation of the nuclear factor – erythroid 2-related factor 2 (NRF2) – a transcription factor involved in redox metabolism, as for example antioxidant responses (65).

Phosphorylation of eIF2α allows the translation of Activating Transcription Factor (ATF4) mRNA, which encodes a transcription factor controlling the transcription of genes involved in autophagy, apoptosis, amino acid metabolism and antioxidant responses (66).

Studies in humans, investigations using PERK−/− mice and mice (Ser51Ala) with a mutation in the phosphorylation site of eIF2α showed a potential relationship between ER stress and β-cell function (67) (68). It suggests that lack of PERK leads to severe cell dysfunction and diabetes (67). Moreover, activation of heterozygous eIF2α mutant mice on a high-fat diet causes distension of the ER lumen in cells, a reduction in islet insulin content and diabetes (69). Also, endoplasmic reticulum (ER) stress is considered a major alteration in obesity, leading to suppression of insulin receptor substrate-1 (IRS-1) signaling, mediated by hyper-activation of the c-Jun N-terminal kinase (JNK) and subsequent serine phosphorylation (70).

b) The Inositol-Requiring Enzyme 1 (IRE1) Pathway

The IRE1 exists in the mammalian genome in two isoforms, IREα (it has been the subject of more studies) and IREβ (71).

Engagement of 'alarm stress pathways' by UPR sensors may modulate ER stress adaptation, apoptosis or physiological outputs that are not directly related to protein-folding stress. For example, activation of IRE1α can activate alarm genes by recruiting the adaptor protein TNFR-associated factor 2 (TRAF2). This results in the activation of the apoptosis signal-regulating kinase 1 (ASK1; also known as MAP3K5) pathway and its downstream target JNK (71). JNK regulates and activates apoptotic pathways and can also contribute to necrosis in response to ER stressors. The JNK branch of the IRE1 pathway can promote cell death.

It is still not known whether the function of the IRE1 pathway *in vivo* is generally pro-death or pro-survival. The RNAse activity of IRE1 can take a role in RNA degradation to reduce protein synthesis, a process known as regulated IRE1-dependent mRNA decay (RIDD). Among these, the transcription factor X-box-binding protein 1 (XBP1) is particularly important for cell survival. The mRNA of XBP1 is synthesized as a nonspliced, untranslated form (uXBP1). When IRE1 is activated it removes a small intron resulting in the formation of spliced XBP1 (sXBP1). This splicing is commonly used as a readout of UPR activation. sXBP1 is a marker and a key regulator of the UPR, as it transcriptionally activates a several genes responsible for restoring ER folding capacity (57). Studies reported Huntington's disease as a neurodegenerative disease involving the accumulation of large-protein inclusions generated by mutant huntingtin protein leading to upregulation of XBP1s in the striatum of patients (72).

c) The Activating Transcription Factor 6 (ATF6) Pathway

ATF6 is a basic Leucine zipper (bZIP) transcription factor in its cytosolic domain and bounds to the ER membrane in unstressed cells. ATF6 has two isoforms, ATF6α and ATF6β. Both are ubiquitously expressed. It is activated by its release from coat protein (COII) complex, which allows it to translocate to the Golgi system. There, it is cleaved by local proteases (S1 and S2 proteases) releasing the active fragments into the cytoplasm from where it is transported to the nucleus. In the nucleus, the active fragments of ATF6f bind specific sequences in promoter regions, ER stress response elements in target genes. A key target of ATF6f is the x-box binding protein-1 (XBP-1) (44). In addition, during tumour growth, several ER stress activators (hypoxia and low glucose) induce resistance to chemotherapy by processes that are suggestive of ER-dependent mechanisms (73). More significantly, a downstream transcriptional target of ATF6α – Binding immunoglobulin Protein (BiP), was described to serve as a malignancy marker for cells. Upon induction of ER stress, ATF6α rapidly induces BiP expression, which binds to unfolded protein and misfolded protein to improve ER stress. In normal conditions, BiP is localized in ER lumen, but upon overexpression, in many types of human cancer, it becomes detectable on the cell surface (73,74). Its expression, not only correlates with cancer, cell proliferation and histological grade but also correlates with therapies and prognosis response (75).

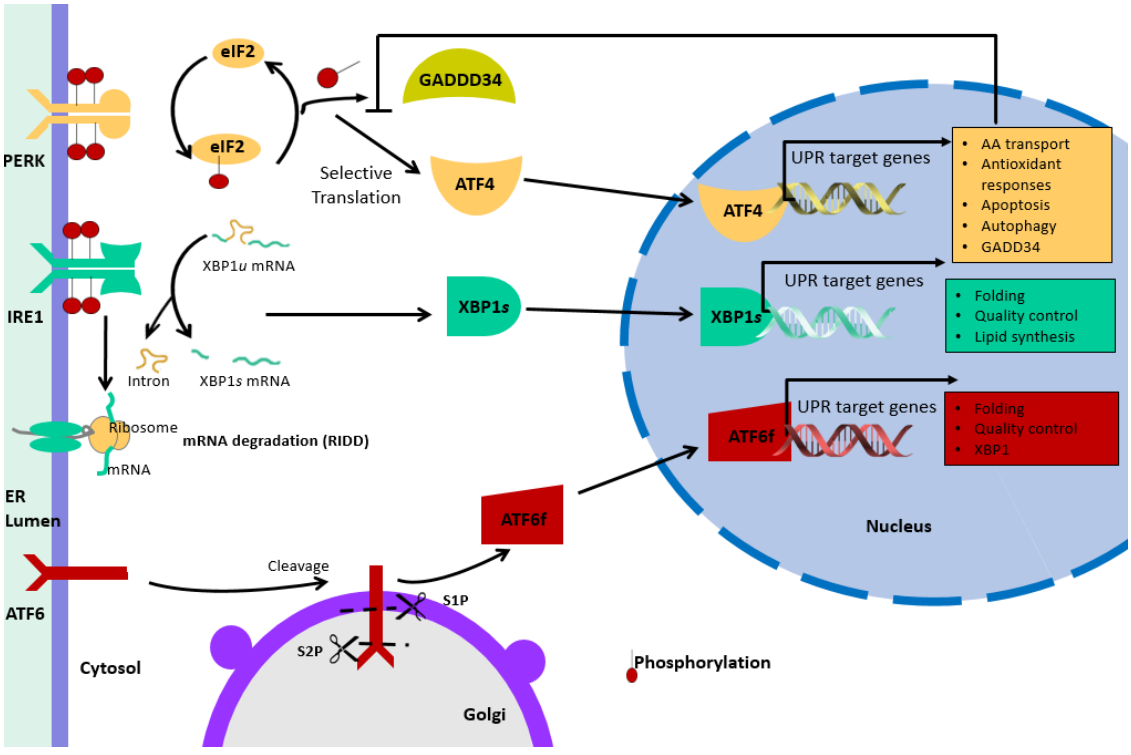

Figure 8: The three processes involved in activation of the UPR response. The three main sensors of the UPR are PERK, IRE1 and ATF6. Adapted from: (76).

1.3.3 Ubiquitin Proteassome Pathway (UPP)

In 2004, Avram Hershko, Aaron Ciechanover and Irwin Rose received the Novel Prize in Chemistry for the discovery and characterization of the ATP-dependent, ubiquitin-mediated protein degradation pathway, unraveling the central role of the Ubiquitin proteasome pathway (UPP) in biology (77).

Ubiquitin is a highly conserved 76-amino acid protein that can be covalently linked to many cellular proteins by the ubiquitination process. Ubiquitylation (also known as ubiquitination) is a process carried out by three classes of enzymes: "ubiquitin activating enzyme" (E1); "ubiquitin-conjugating enzyme" (E2) and "ubiquitin ligase" (E3). The E1 forms a thio-ester bond with ubiquitin; this reaction allows subsequent binding of ubiquitin to E2, followed by the formation of an isopeptide bond between the carboxy-terminus of ubiquitin and the ε-amino group of a lysine residue on the substrate protein. The latter reaction requires the E3 which can only modify a subset of substrate proteins, thereby providing substrate specificity to the system. Ubiquitinated proteins are then targeted to the 26S proteasome for degradation or experience changes in protein location or activity (78). Deubiquitinating enzymes (DUBs) reverse the process of ubiquitination by removing ubiquitin from its substrate protein. DUB activity sustains ubiquitin recycling and ensures that ubiquitin molecules remain steady. DUBs are categorized into 5 subfamilies: USP, UCH, OTU, MJD, and JAMM, with a specific tissue and substrate, each (79).

The UPP is a process involving two steps: first, the marking of the substrate protein is made by the covalent attachment of multiple ubiquitin molecules – Conjugation; and second, these proteins are then transported to the 26S proteasome, composed by the catalytic 20S core and the 19S regulator, where they are degraded – Degradation. This classical function of ubiquitin is associated with housekeeping functions, regulation of protein turnover and antigenic-peptide generation (80).

The 26S proteasome is a highly abundant complex that serves as the proteolytic arm of the ubiquitin-proteasome system. It is composed by two sub-complexes, the 19S regulatory particle (RP) – that includes a base and a lid – and the 20S catalytic core particle (CP), forming an empty cylindrical structure. The base is formed by six proteins with ATPase activity (Rpt1-Rpt6), and four proteins lacking ATPase activity (Rpn1, 2, 10, 13).

Its functions are to unfold the substrate and allow the access of the unfolded substrate into the catalytic chamber.

The lid is mainly involved in specific recognition of the ubiquitin signal. In addition to the 19S cap, other proteins and complexes bind to the end of the 20S cylinder and activate it by

facilitating the opening of the gate. The 20S catalytic subunit consists of seven different protein subunits. Two rings of subunits denominated alfa (α1 -7) located at the ends of the cylindrical structure. The other two rings of subunits called beta (β1-7) are located in the central area (79) (81).

More recently, it has become evident that protein modification by ubiquitin also has unconventional functions (non-degradative) such as the regulation of DNA repair and endocytosis. These functions are determined by the number of ubiquitin units attached to proteins (mono *versus* poly-ubiquitination) and also by the type of ubiquitin chain linkage (82).

Several cellular processes are regulated by ubiquitin-mediated proteolysis, such as elimination of misfolded or damaged proteins, apoptosis, biogenesis of organelles, cell cycle and division, DNA transcription and repair, differentiation and development, immune response and inflammation, neural and muscular degeneration, morphogenesis of neural networks, modulation of cell surface receptors, ion channels and the secretory pathway, response to stress and extracellular modulators, ribosome biogenesis, viral infection and so one (83). All major human chronic neurodegenerative diseases, such as Parkinson Disease (PD), AD, Huntington Disease (HD) and ALS, are characterized by ubiquitinated proteins that are accumulated in abnormal intraneuronal inclusions in the respective affected areas of the Central Nervous System (CNS) (84).

1.3.4 Autophagy

Autophagy is a dynamic and continuous process that degrades cytoplasmic contents, misfolded proteins, and excess or damaged organelles, essential for survival, differentiation, development and homeostasis. This *self-eating* process, involves the appropriation of cytoplasmic components by a small portion of the membrane, creating an autophagosome. So they are fused to the lysosomes, creating an autolysosome, resulting in degradation of cellular components *via* lysosomal enzymes (85). Furthermore, autophagy has been described as being generally activated by conditions of nutrient deprivation or invading organisms but has also been associated with physiological and pathological processes, as well, such as neurodegeneration, stress, heart disease, obesity, and cancer (86).

Mammalian autophagy is a process that involves several components, such as the autophagy-related 1 (Atg1)/unc-51-like kinase (ULK) complex; two transmembrane proteins, Atg9 and vacuole membrane protein 1 (VMP1); proteins that lead to fusion between autophagosomes and lysosomes (87); Beclin 1 and other components in the class III

phosphatidylinositol 3-kinase complex (PtdIns3K); and finally, two ubiquitin-like proteins conjugation systems (Atg12 and Atg8/LC3) (88).

Three different types of autophagy co-exist in most types of mammalian cells, according to the molecular components involved (86):

Macroautophagy involves the appropriation of cytosolic regions by a *de novo* formed membrane that covers into double-membrane vesicles (autophagosomes) for delivery to lysosomes through vesicular fusion, required for the content degradation. Induction of macroautophagy leads to the mobilization of a protein kinase type III complex – the initiation complex – towards the autophagosome formation. Lipid phosphorylation of this kinase complex is essential for the mobilization, in these regions, of the components of two conjugation cascades that mediate formation and elongation of the autophagosome membrane. The major negative regulator of macroautophagy – the mTOR protein kinase complex – is also there (89);

Microautophagy, the cytosolic content, is internalized for degradation in single-membrane vesicles that are made by invaginations in the surface of lysosomes or late endosomes. The molecular components that play a role in this autophagic process in mammals remain unknown (90);

Chaperone-mediated autophagy (CMA) differs from the other autophagic pathways on the fact that substrates – only soluble cytosolic proteins – are selectively targeted to the lysosomal membrane by a cytosolic chaperone and they require unfolding before reaching the lysosomal lumen. Internalization of substrate proteins by this pathway is attained by the coordinated function of chaperones at both sides of the lysosomal membrane and a membrane protein – the lysosome-associated membrane protein type 2A or LAMP-2A – that act both as receptor and as an essential component of the translocation complex (90).

These types of autophagy differ in the mechanisms that mediate the delivery of content to lysosomes. They regulate the subset of genes and proteins that act as effectors and modulators, in each of them (88). On the other hand, loss of this mechanism leads to alteration in protein quality control, disruption metabolic homoeostasis, and inefficient stress response, with a negative impact on mammalian homeostasis (91).

1.4 Aggregation reporter systems

A HSP27-GFP reporter system was developed to monitor general protein aggregation in HeLa cells by our group. To construct this, human HSP27 promotor and coding region were cloned from HeLa cells and fused with Green Fluorescent Protein (GFP). A HeLa stable cell line expressing this reporter was generated after transfection of the plasmid containing the HSP27-GFP fusion and selection by geneticin (G418). GFP was used to monitor the HSP27 expression. In a normal situation, cells expressing the HSP27-GFP sensor exhibit a general and homogenous green fluorescence, as HSP27 is ubiquitously expressed even in unstressed cells. In situations where misfolded proteins are present, the GFP fluorescence is re-localized to foci, corresponding to the recruitment of HSP27 to help in the refolding of those proteins, as explained above. Thus, the cellular re-localization of this aggregation reporter fluorescence to foci can identify situations where protein misfolding is occurring.

Having a stable cell line expressing this reporter is essential to perform genetic screenings to identify genes involved in proteostasis. Genetic screenings are based on the small interfering RNA (siRNA) technology.

siRNAs are small non coding RNA molecules that block translation by binding to complementary sites on mRNAs. The siRNAs are generated from double stranded RNA (dsRNA) precursors by cleavage of RNase-III-type enzyme termed Dicer. This enzyme can cleave long dsRNA into 21-28 nucleotide siRNA double-stranded. In this process, more efficiently, the 5´end of antisense strand of the siRNA becomes a part of a multiprotein complex named RNA-induced silencing complex (RISC) (92,93). The RISC identifies the target mRNAs by complementary base-pairing, and cleaves it at a specific site. After degradation of mRNA, the expression of corresponding protein is reduced (92). In mammalian cells, upon transfection of gene-specific siRNA, particular messages are destroyed resulting in a decrease of the corresponding protein level. This knockdown facilitates functional analysis of a gene product in the equivalent cells (94). This is why siRNAs are a powerful research tool when evaluating many proteins expression, dissection the function of independent genes and potential for therapeutic applications (95).

After a literature review, most of the current reporters described for misfolding protein detection are specific for a particular protein (96–99). The recently development, the ProteoStat® Aggresome Detection Kit is indicated to detect aggregated proteins inside aggresomes and inclusion bodies, as storage depots for cargo awaiting degradation by the autophagy system (96). Another developed sensor using split-luciferase complementation assay only allows the monitoring of Aβ oligomers characteristic of Alzheimer's disease (98). Also, a

Luciferase-based protein aggregate reporter was developed to assess specifically polyQ aggregates, a common pathologic feature in neurodegenerative diseases (99). Considering the improved interest in detection and quantification of protein aggregation in mammalian cells, the development of alternative and more general molecular folding reporters is needed.

Indeed, our HSP27-GFP reporter is unique in assessing general protein aggregation and offers advantages over other mentioned reporters. Using an endogenous source, HSP27 is a small heat shock protein family (sHSPs) that binds to any unfolded proteins until the refolding action by ATP-dependent heat shock proteins. Furthermore, this molecular chaperone is over-expressed in stressful situations, and have anti-apoptotic and anti-oxidant functions, particularly in pathological conditions (100–102).

1.5 Motivation and aims of the study

Protein conformational diseases have been the subject of several studies performed within the past 20 years and have generated important, and partly addressed here, pieces of knowledge, while a number of questions still remain unanswered. Although the mechanisms associated with the unfolded protein response have been extensively explored, it is crucial to identify which genes contribute to protein aggregation. The growing number of tRNA-modifying enzymes implicated in a large number of diseases, in particular in conformational disorders, suggests that these molecules play important roles in proteostasis. There is a lack of experimental demonstration that proves the association between tRNA modifying enzymes, protein aggregation and the underlying mechanisms that lead to the onset of disease. We hypothesize that deregulation of tRNA-modifying enzymes, in particular the ones that affect translation fidelity, results in protein aggregation and activation of UPR, which are characteristic of conformational disorders. In order to test this hypothesis, we implemented a fluorescent method based on small interfere RNA (siRNA) screening, aiming to identify the human tRNA modifying enzymes responsible for homeostasis of the proteome.

To monitor protein aggregation, we used an immortalized cell line – HeLa cells – stably expressing the reporter system HSP27-GFP previously developed by the members of the laboratory. In this thesis, it is demonstrated that the stable cell line expressing the protein aggregation reporter can be used to monitor situations where misfolding proteins accumulate in cells. Also, a fluorescent siRNA based screening of particular tRNA modifying enzymes, namely, Elongator complex protein 3 (ELP3) and Alkylated DNA repair protein alkB homolog 8 (ALKBH8) was performed. ELP3 was identified as an enzyme involved in protein aggregation and additional experiments demonstrated that deregulation of this enzyme leads to alterations at the level of protein synthesis and increased ubiquitination, showing that this enzyme is essential for proteostasis. Taken together, the data collected in this thesis demonstrates that the initial hypothesis was correct and additional experiments are now undergoing to identify others enzymes involved in proteostasis and to further dissect the molecular consequences of ELP3 deregulation.

CHAPTER 2.

Materials and methods

2.1.1. Cell culture

A stable HeLa cell line, expressing the fluorescent reporter HSP27-GFP, was cultured in Dulbecco's Modified Eagle Medium (DMEM), supplemented with 10% of Fetal Bovine Serum (FBS) and 1% of Pen-Strep-Glut (a mixture of the antibiotics penicillin and streptomycin, and the amino acid glutamine). These cells were maintained in culture, in an incubator at 37 °C with 5% CO_2 and 95% of humidity. For all assays, except fluorescence and proteostat, cells were detached from the plates with TrypLE Express (ThermoFisher Scientific), a trypsin alternative, and incubated 5 minutes at 37 °C. Next, the resultant cell suspension was centrifuged for 3 minutes, at 3000 rpm, at Room Temperature (RT). Then, the supernatant was discarded and the pellet was ressuspended in fresh medium. 2µL of suspended cells were diluted in 18 µL of trypan blue followed by cell counting in a Neubauer chamber. Additionally, the experiments with MG132 (carbobenzoxy-Leu-Leu-leucinal were performed after incubating cells with 5µM of MG132 for 18 hours.

2.1.2. Total protein extraction and quantification

To obtain total protein extracts, pellets were ressuspended in 100 µL of Empigen Lysis Buffer (ELB – Annexes). Protein extracts were then sonicated for 2 cycles, at a 60% frequency, during 15 seconds each, and centrifuged 20 minutes at 200*g* at 4 °C. In the end, supernatants were kept for the next phase of total protein quantification. During all procedures, cells remained on ice to avoid the activity of proteases. Quantification of total protein was performed using Pierce™ Bovine Serum Albumin (BCA) Protein Assay Kit (Thermo Scientific), following the manufacturer´s instructions. The total extracts were incubated with the BCA reagent for 30 minutes at 37 °C, followed by absorbance measurement at 575 nm in a microplate reader.

2.1.3. Insoluble protein fraction

To isolate the insoluble protein fraction, the volume corresponding to 200µg of total protein was diluted in ELB to reach a final volume of 100µL. Samples were centrifuged in a micro-centrifuge (16,000*g*, 20 minutes) at 4 °C to obtain the insoluble fraction. The resulting pellet was solubilized in 80 µL of ELB and 20 µL of NP40 (10%). Samples were sonicated for 20 seconds (three times). After sonication cycles, samples undergone another centrifugation (16,000 *g*, 20 minutes at 4 °C). The supernatant was removed, the pellet was washed with 50µL of ELB and sonicated for 10 seconds (0,5 cycles with frequency at 50-60%). Finally, a loading buffer was

added (10µL of 6x SDS), and samples were denatured at 95 °C during 5 minutes. For SDS-PAGE, 30µL of sample were added in each well in the acrylamide gel (10%).

2.1.4. SDS-PAGE and Western Blot

To perform Western Blot analysis, proteins were allowed to migrate through Sodium Dodecyl Sulfate-Polyacrylamide Gel Electrophoresis (SDS-PAGE). A concentration in a range of 10-20 µg of total protein was loaded in the polyacrylamide gel (10%), according to the quantity measured in the BCA Protein Assay Kit. Samples were prepared with 6x concentrated protein loading buffer and then denatured at 95 °C for 5 minutes. The gel was loaded with a molecular marker (Nzy Colour Protein Marker II) in the first well followed by the samples, and then, 1x concentrated Running Buffer was added to the electrophoretic container to immerse the running gel. SDS-PAGE ran for 2 hours, first at 80 V for 15 minutes to allow the samples to pass through the stacking gel, and then at 110 V (Annexes - solutions). Next, proteins were electro transferred onto a nitrocellulose membrane in the Trans-Blot® Turbo™ Transfer System for 7 minutes. The membrane was blocked in 5 or 2% Bovine Serum Albumin (BSA) [diluted in tris-saline buffer with tween 20 (TBS-T)] and incubated with the primary antibody for 2 hours (Table 3). The blots were then washed three times for 5 minutes each with TBS-T and then incubated with the respective secondary antibody (Table 3) for 1 hour at RT, protected from light. Membranes were washed twice with TBS-T for 5 minutes and once with 1x TBS for 5 minutes. The membranes were digitalized in the Odyssey scanner and analyzed in its software (LI-COR, Biosciences, US). This system is equipped with two infrared channels for direct fluorescence detection on membranes (700 and 800 nm, anti-rabbit and anti-mouse respectively).

Table 3: Antibodies used for Western Blot analysis.

Primary Antibody	**Host**	**Secondary Antibody (1:10 000)**
Anti-Hsp27 (1:1000) StressMarq Biosciences	Mouse	Anti-Mouse IRDye®800CW LI-COR
Anti-BiP (1:1000) StressMarq Biosciences	Rabbit	Anti-Rabbit IRDye®680LT LI-COR
Anti-Ubiquitin (1:1000) Sigma	Mouse	Anti-Mouse IRDye®800CW LI-COR
Anti-ATF6 (α) (1:400) Stressgen	Mouse	Anti-Mouse IRDye®800CW LI-COR
Anti-eif2α (1:1000) Cell signaling	Rabbit	Anti-Rabbit IRDye®680LT LI-COR
Anti-eif2α-P (1:4000) Abcam	Rabbit	Anti-Rabbit IRDye®680LT LI-COR
Anti-GADPH (1:1000) Abcam	Rabbit	Anti-Rabbit IRDye®680LT LI-COR
Anti-β-tubulin (1:1000) Invitrogen	Mouse	Anti-Mouse IRDye®800CW LI-COR

2.1.5. Reverse transfection with siRNA

siGenome SMARTpool human siRNA targeting different tRNA modifying enzymes were obtained from Dharmacon (Thermo Scientific) and reverse transfected into the stable HSP27-GFP HeLa cell line in 24 well plates (Table 4). Briefly, 12 µL of 500 nM siRNA duplex in 88µL of Opti-MEM were added to each well, followed by addition of 1µL/well of the mix of lipofectamine RNAi max. After an incubation for 30 minutes $2x10^4$ cells were added to each well in complete growth medium without antibiotics. Finally, the cells were incubated for 48 or 72 hours at 37 °C in a CO_2 incubator.

Table 4: tRNA modifying enzymes tested (based in table 10- Annexes).

Human tRNA modifying enzyme	Modification
IKBKAP	mcm^5U_{34}, $mcm^5s^2U_{34}$, ncm^5U_{34}, ncm^5Um_{34}
Elp2	mcm^5U_{34}, $mcm^5s^2U_{34}$, ncm^5U_{34}, ncm^5Um_{34}
ELP3	mcm^5U_{34}, $mcm^5s^2U_{34}$, ncm^5U_{34}, ncm^5Um_{34}
Elp4	mcm^5U_{34}, $mcm^5s^2U_{34}$, ncm^5U_{34}, ncm^5Um_{34}
Elp5	mcm^5U_{34}, $mcm^5s^2U_{34}$, ncm^5U_{34}, ncm^5Um_{34}
Elp6	mcm^5U_{34}, $mcm^5s^2U_{34}$, ncm^5U_{34}, ncm^5Um_{34}
KTI12	mcm^5U_{34}, $mcm^5s^2U_{34}$, ncm^5U_{34}, ncm^5Um_{34}
URM1	$mcm^5s^2U_{34}$
CTU2	$mcm^5s^2U_{34}$
CTU1	$mcm^5s^2U_{34}$
TRMU	tm^5U_{34}, $tm^5s^2U_{34}$
NSUN2	m^5C_{34}, m^5C_{40}, m^5C_{48}, m^5C_{49}
ALKBH8 (TRM9)	mcm^5U_{34}, $mcm^5s^2U_{34}$
FTSJ1	Cm_{32}, Cm_{34}, Gm_{34}, ncm^5Um_{34}
Qtrt1	Q_{34}
TRDMT1	m^5C_{34}

2.1.6. Immunocytochemistry - Proteostat

Cells were plated on coverslips and treated with negative and positive controls and incubated with Proteostat Aggresome Dectetion kit (Enzo Life Sciences International), according with the manufacturer's instructions. Briefly, cells were washed three times with phosphate buffered saline (PBS) and fixed with a 4% of paraformaldehyde solution (PFA) for 30 minutes at RT. After that, the coverslips were washed three times with PBS and cells were incubated with a Permeabilizing Solution (100mL PBS + 1mL glycine (1M) + 5% FBS + 0.1% Triton) for 30 minutes. The cells were washed three times with PBS, before and after, an incubated (in darkness) with the Dual Detection Reagent, for 30 minutes at RT. Finally, the coverslips were mounted on microscope slides using mounting medium and were observed under a fluorescence or a confocal microscope. The resulted images were analysed via ImageJ.

2.1.6.1. Mitotracker Red CM-H2XROS

A working solution of 200 nM in cell medium was obtained from 1 mM Mitotracker stock solution prepared in dimethylsufoxide (DMSO). Mitotracker staining solution was added to the cells after changing the growth medium by Mitotracker working solution. After an incubation of 30 minutes, cells were washed with fresh medium and fixed in 4% of PFA for 15 minutes. Finally, the cells were rinsed 3 times in PBS and coverslips mounted and observed in a Zeiss epifluorescence microscope.

2.1.7. Confocal and fluorescence microscopy

Cells were plated in 24 well plates containing coated coverslips (Corning) at a $2x10^4$ cells/mL cellular density and transfected as detailed in 2.1.5 or treated as detailed in 2.1. All cells were then fixed with a solution containing 4% of PFA and incubated for 15 minutes at RT. Some coverslips were treated with PROTESOSTAT– as detailed in 2.1.6 or incubated with DAPI for 15 minutes at RT. Coverslips were washed 3 times with PBS and mounted on a glass slide with Vectashield mounting medium. Slides were dried in the dark and then observed in the Olympus IX-81 confocal microscope, for confocal microscopy experiments or in the Zeiss Axioimager for fluorescence microscopy.

2.1.8. Cellular viability assay

To determine cell viability the colorimetric MTT (3-(4,5-dimethylthiazol-2-yl)-2,5-diphenyltetrazolium bromide), metabolic activity assay was used. Hela HSP27-GFP control and transfected cells (1×10^4cells/well) were cultured in a 96-well plate at 37 °C. The supernatant of each well was removed and washed twice with PBS, 12,5 µl of MTT solution (5 mg/mL in PBS) and 100µl of medium were then added. After an incubation of 2 hours, the resultant formazan crystals were dissolved in dimethyl sulfoxide (100µl) and the absorbance intensity was measured by a microplate reader (Bio-RAD) at 575 nm. Cells treated with medium only worked as a negative control group. Positive and negative siRNAs controls were used. All experiments were performed in triplicated, and the relative cell viability (%) was expressed as a percentage relatively to the untreated control cells.

2.1.9. RNA extraction

The RNA was extracted using the NZY Total RNA Isolation kit and the manufacturer's protocol was followed. Briefly, before starting the RNA isolation, a Digestion Mix with DNase I and a digestion buffer were prepared. Next, a buffer NR and β-mercaptoethanol was added to the cells' pellet and vortexed vigorously. These solutions were applied to an NZYSpin Homogenization column placed in a 2mL collection tube, followed by centrifugation (11000*g*, 1 minute), in which the flow-through was saved. The lysate was pipetted and loaded in an NZYSpin Binding column and, centrifuged (11000*g*, 1 minute). The flow-through was discarded and the column placed into a new collection tube. The Buffer NI was added, the samples centrifuged and the flow-through was discarded and placed in the column back into the collection tube. In this moment, the Digestion Mix was applied and incubated at RT for 15 minutes. The Buffer NWR1 and NWR2 were added, respectively, centrifuged and the flow-through was discarded and the column was placed in a new collection tube. 30µL of RNase-free water was added directly in the column membrane and centrifuged (11000*g*, 1 minute) to elute the RNA. RNA was stored at -20 °C for short-term or at -70 °C for long-term and quantified in a Denovix spectrophotometer.

2.1.10. cDNA synthesis

cDNA was synthesized from total RNA using the High Capacity cDNA Reverse Transcription kits (Applied Biosystems), according to manufacturer´s instructions. Briefly, three major steps were followed in order to synthesize single-stranded cDNA:

i. 2x Reverse Transcription master mix was prepared, as described in the table 5, using the kit components.

ii. Addition of 10µl of total RNA (100 ng/µL) to the previous master mix (step I) in order to create a 1x mix.

iii. The settings applied in the thermal cycler for the reverse transcription were: step 1: 25 °C for 10 minutes; step 2: 37 °C for 2 hours; step 3: 85 °C for 5 minutes and 10 °C.

Table 5: Reverse Transcription master mix preparation.

Components	**Volume/Reaction (µL)**
10x RT Buffer	2,0
25x dNTP mix (100mM)	0,8
10x RT Random Primers	2,0
MultiScribe Reverse Transcriptase	1,0
Nuclease- free water	4,2
Total per Reaction	10

2.1.11. Real-Time Polymerase Chain Reaction (RT-PCR)

Expressions of the ELP3, ALKBH8 and GADPH genes were analyzed by Real-Time Polymerase Chain Reaction (RT-PCR), using specific TaqMan probes obtained from Thermo Fisher Scientific and the components described in table 6. The thermal cycle profile of the qPCR machine was set-up as shown in table 7 and the experience was performed in an ABI Prism 7500 Real-Time PCR System (Applied Biosystems), containing a 96 well block.

Table 6: Real time PCR reaction mix.

Components	Volume/Reaction (µL)
20x TaqMan® Gene Expression Assay	1
2x TaqMan® Gene Expression Master Mix	10
cDNA (100ng/ µL)	4
RNase- free water	5
Total volume/well	20

Table 7: Thermocycler programmer (40x) – Standard Conditions.

Fases	Temperature	Duration
Initial denaturation	50°C	2’
Denaturation	95°C	10’
Annealing	95°C	15’’
Extention	60°C	1’
Final Extention	4°C	∞

2.1.12. SUnSET method

To estimate protein synthesis rate, the SUnSET method was used. This technique required the incubation of cells with 5 µL of puromycin (10 µL/mL) for 15 minutes. Next, the cells were fixed for 15 minutes with PFA 4% and washed twice with PBS and centrifuged (3000 *g*, 3 minutes at 4 °C). Cells were ressuspended in 200 µL of cytometric fluid and 10 µL were removed from each sample and mixed in a tube as a baseline. The tube´s content was placed into the plates or Eppendorf’s tubes to be centrifuged and washed once. Cells were incubated with an anti-puromycin antibody (dilution of 1:1000) for 1 hour at RT protected from light. Next, 50 µL of cytometry buffer was added followed by centrifugation and the supernatant was removed. 200µl of cytometry buffer was added and another cycle of centrifugation was performed. Two wash steps with 300 µL PBS were followed. Cells were analyzed with a flow FITC cytometer detector using the FL1-A (puromycin) and FL4-A (GFP) channels.

2.1.13. Statistical analysis

Statistical analysis were performed in the GraphPad Prim® v5.01 software, using Student´s t-test (paired t test), except for the results of RT-PCR that were assessed by unpaired t test. The results were presented as means values of the number of experiments.

CHAPTER 3.

Results

3.1.1. Evaluation and optimization of the HeLa HSP27-GFP stable cell line

In order to monitor protein aggregation *in vivo* a HeLa stable cell line expressing the HSP27-GFP chimeric reporter protein was generated in our laboratory. The validation of the HSP27-GFP reporter has been previously confirmed by transient transfections prior to the beginning of this thesis and the stable cell line was established before as well. The work developed in this thesis begun by testing the efficiency of the HSP27-GFP sensor expressed in the stable cell line. For that, HeLa cells and HeLa HSP27-GFP cells were plated in 6 multi well plates at a $2x10^5$ cells/mL density and the reporter expression in the stable cell line was confirmed by western blotting, as shown in figure 9.

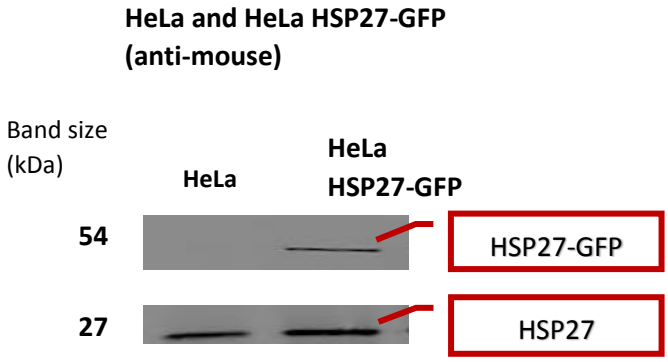

Figure 9: Stable cell line expressing HSP27-GFP fusion sensor. HSP27-GFP system was transfected in HeLa cells using lipofectamine 2000. Stable clones were selected by G418 and expanded.

As expected, in control HeLa cells (not expressing the reporter), HSP27 was detected as a band of ~27KDa, as this chaperone is ubiquitously expressed even in non-stressful situations whereas in the stable cell line expressing the HSP27-GFP fusion, a band of ~27KDa is detected together with a bigger band, of ~54KDa, that corresponds to the expected size of the fusion of HSP27-GFP (both HSP27 and GFP are 27 kDa) (Figure 9). Western blots for GFP were also performed. In this case, HeLa cells not expressing the reporter did not express GFP (no band was detected), whereas in the stable cell line a band of ~54KDa was observed, as expected. No free GFP was detected as cells did not express free GFP (data not shown).

In order to test its efficiency, these stable cell lines were incubated with MG132, a proteasome inhibitor commonly used as a positive control to test for protein aggregate accumulation. As the proteasome is inhibited, cells cannot degrade the potential erroneous proteins that are synthesized and as a consequence they accumulate in cells. As expected, after incubation with MG132 re-localization of GFP fluorescence to *foci* was observed in the stable

cell line, when compared with the control condition where HeLa HSP27-GFP cells were grown in complete medium, displaying a homogeneous GFP expression and no aggregation (Figure 10).

To further verify that the sensor was working as expected in the stable cell line, we also tested the PROTEOSTAT® Aggresome Detection kit that has been used in detection of denatured and/or misfolded protein aggregates and inclusion bodies. This kit co-localized with most GFP fluorescence *foci*, indicating that protein aggregation was occurring and the HSP27-GFP sensor expressed by the stable cell line was functional. Based on this data, we proceeded for the siRNA screening of tRNA modifying enzymes using this stable cell line.

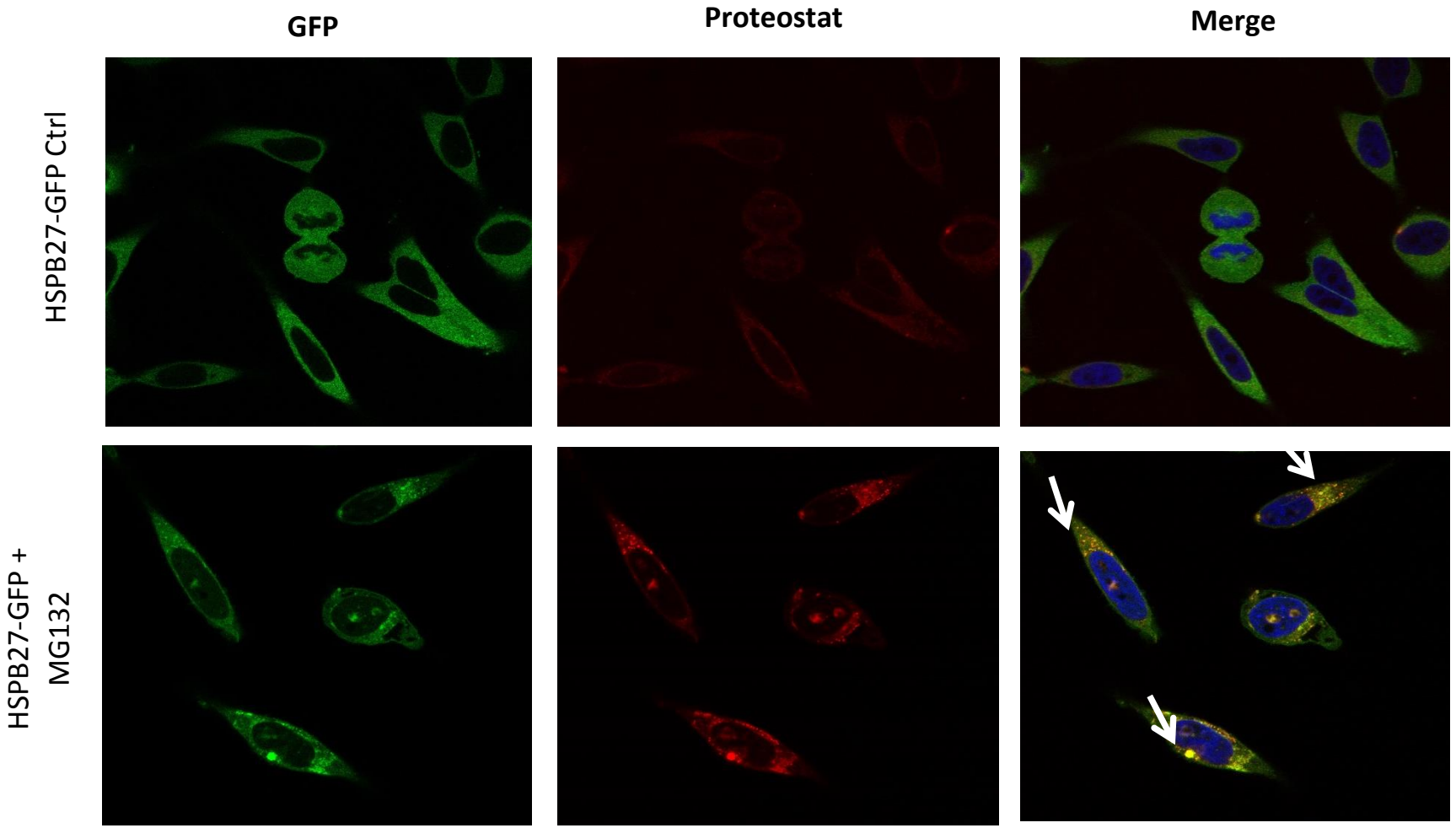

Figure 10: Reporter validation: HeLa HSP27-GFP stable cells were kept in complete medium (Ctrl) or incubated with MG132 for 18 hours to inhibit the proteasome. After incubation cells were washed, fixed and incubated with proteostat, a protein aggregation commercial detection kit. Control cells display a homogeneous HSP27-GFP expression and no aggregation. MG132 exposed cells display re-localization of GFP fluorescence to foci that co-localize with proteostat fluorescence, indicating that protein aggregation is occurring and HSP27-GFP reporter is functional. Hoescht (blue), GFP (green) and Proteostat kit (red). **Confocal fluorescence microscopy**, magnification 63x.

As there was a strong re-localization of fluorescence to *foci* after incubation of the stable cell line with MG132, indicating that there was an accumulation of misfolded proteins in cells where the proteasome was inhibited, we decided to further test if there was an increase in insoluble proteins in cells after treatment with this compound. After isolating the detergent-insoluble protein fraction, we found an accumulation of particular insoluble proteins, indicated by black arrow, in cells exposed to MG132 and not in control cells, corroborating the fluorescence data (Figure 11).

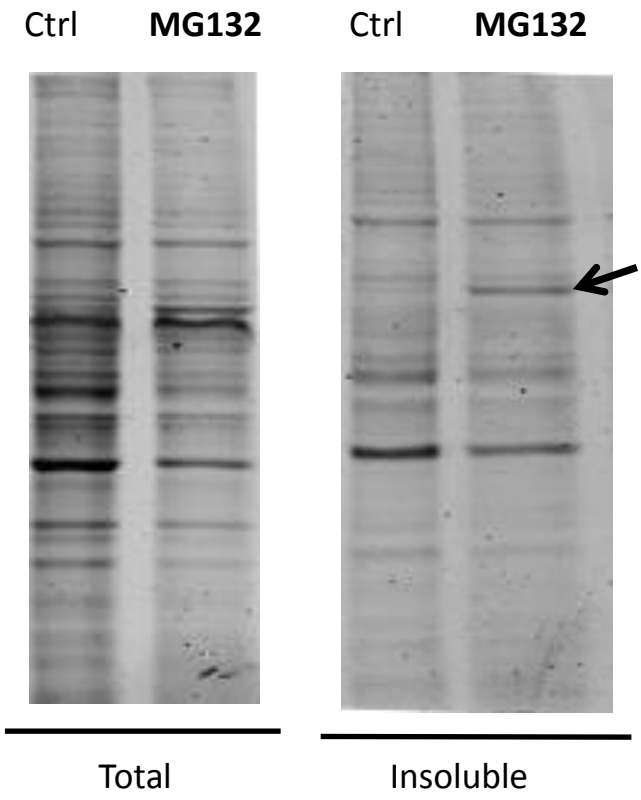

Figure 11: Isolation of insoluble protein fraction: coomassie blue stained SDS- PAGE (10% of acrylamide) of total protein fraction and insoluble (hydrophobic) proteins. In insoluble fraction an extra band was observed (arrow) in cells treated with MG132.

Furthermore, the treatment with MG132 led to an increase in the expression of HSP27, as well as in the expression of, HSP27-GFP, as shown by western blot (Figure 12).

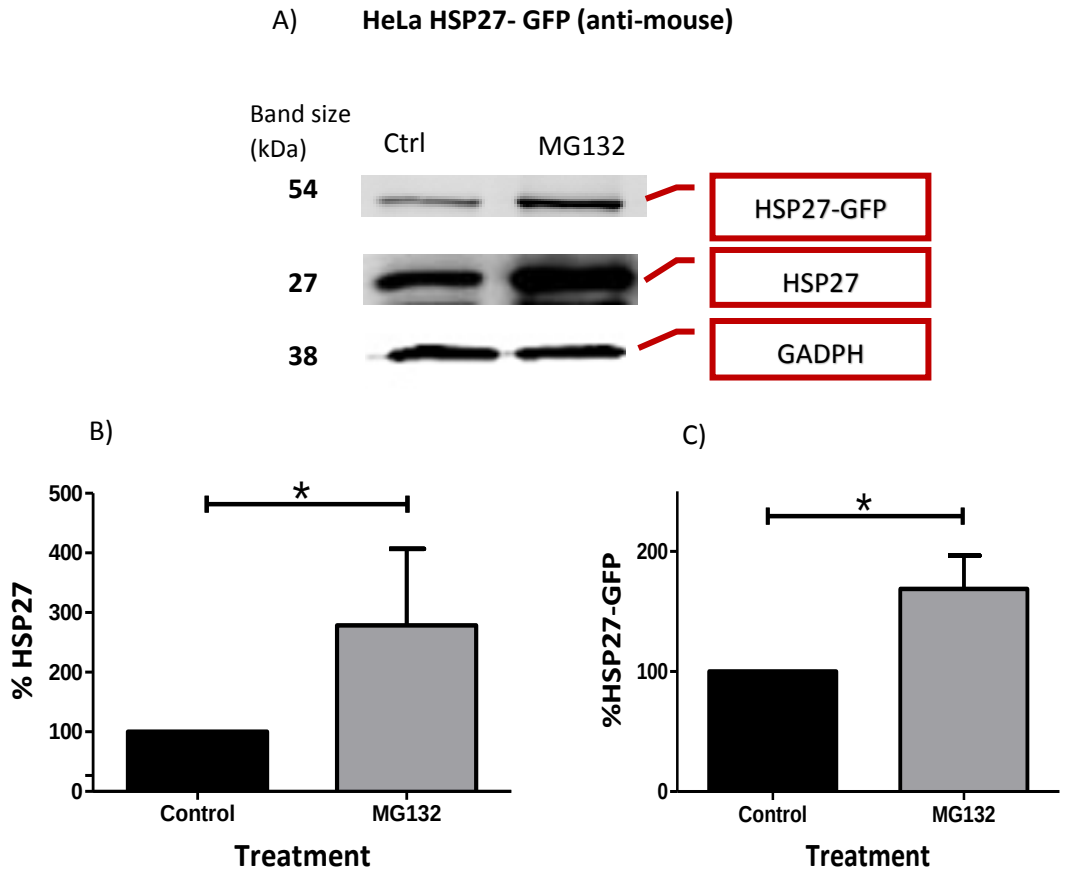

Figure 12: Stable cell line expressing HSP27-GFP fusion selection. A) Reporter fusion and HSP27 expressions were confirmed by western blotting, after incubation with MG132, a proteasome inhibitor. There was a significant increase in both the expression of endogenous HSP27 and the HSP27-GFP fusion in cells incubated with MG132 when compared to the control. B) Graphic of the % of expression of HSP27 in HeLa cells with HSP27-GFP reporter. Statistically significant changes were observed between the control and the cells treated with MG132; C) Graphic of the % of expression the HSP27-GFP reporter; statistically significant changes in HSP27-GFP expression were observed between MG132 treated cells and the control cells. (Data analysis was done using Student's paired t-test, $P < 0.05$ (*) (N = 3)).

3.1.2. Gene-silencing of ELP3, ALKBH8 and GADPH in HeLa cells

We started our tRNA modifying enzyme fluorescent based siRNA screen testing a limited number of siRNAs (siGenome SMARTpool human) targeting tRNA modifying enzymes, namely ELP3 and ALKBH8. Reverse transfections were optimized by transfecting the mentioned siRNAs and siRNA controls. These controls included: a **positive control**, a validated siRNA that targets an abundantly expressed housekeeping (in our case we used GADPH), to measure the efficiency of siRNA uptake into cells; a **negative control**, a siRNA that does not target any gene in the cells, to distinguish sequence-specific silencing from non-specific affects; **mock**, cells only transfected with lipofectamine RNAiMax and **untreated** cells, to determine baseline phenotype, target gene level, and cell viability. Cytotoxicity and silencing efficiency were tested by **MTT and RT-PCR**, respectively (Figures 13 and Figure 14)**.**

The MTT assay showed a slight decrease in viability of mock and control cells (less than 20 %), which indicates that both the transfection agent (lipofectamine RNAiMax) and the control siRNA are non-toxic. The positive control, as expected, had a significant effect on cell viability (~80 % decrease in viability), indicating that the siRNA transfection method was working. We also observed a decrease in the cell viability as an effect of silencing the ELP3 (~34 %), and ALKBH8 (~29 %) enzymes.

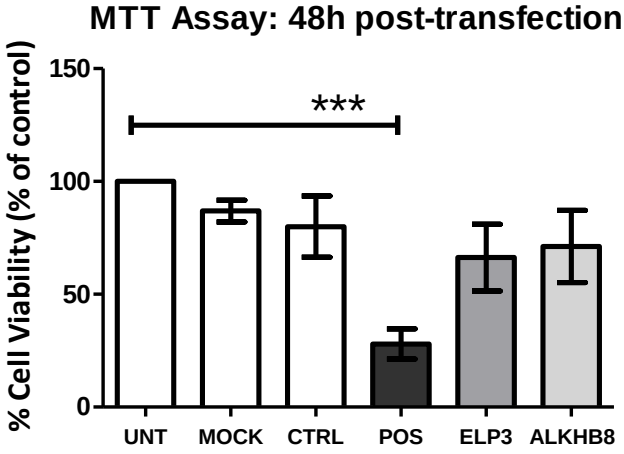

Figure 13: MTT assay, 48 hours after transient transfection of siRNA in the HeLa HSP27-GFP stable cell line. The MTT reduction is measured as absorbance at 575 nm. A significant decrease in the viability of cells was observed for positive control. The viability of mock and control cells has an acceptable decrease (less than 20 %). After siELP3 and siALKBH8 transfection we observed a not statistically significant decrease in the viability of cells. Counts from the experiments performed in triplicate from each group were compared for statistical significance with Student's t test. $P < .001$ was considered highly significant (***) (N = 3).

The efficiency of gene silencing is measured by the percentage of target mRNA reduction in siRNA-transfected cells relative to control-transfected cells. The average transcript levels from four independent siRNA transfection experiments are shown in the figure 14. The cells transfected with the siRNA for ELP3 and ALKBH8 showed clearly a significant downregulation in mRNA expression for which condition.

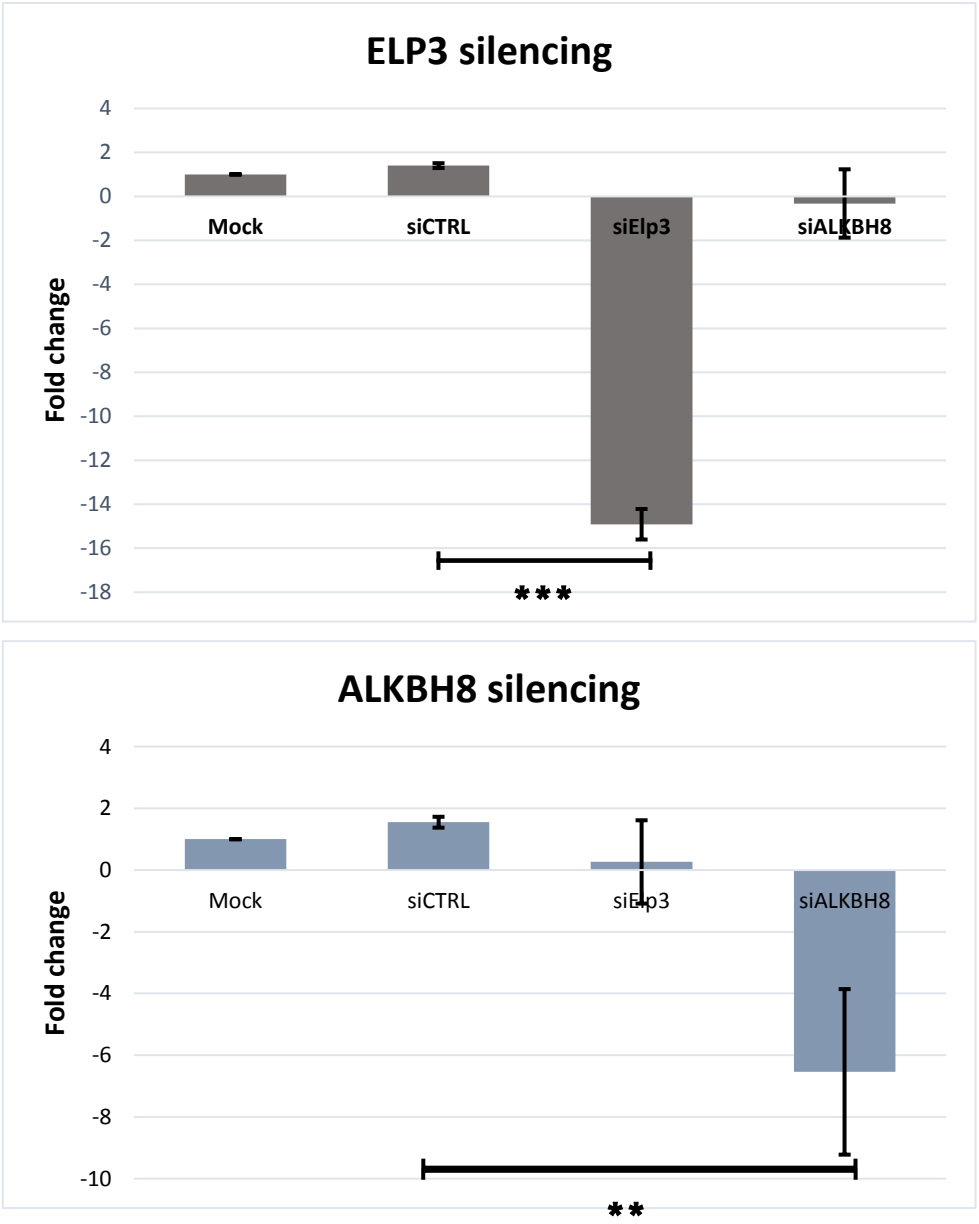

Figure 14: Validation of gene silencing (siRNA) effect performed by Taqman real-time RT-PCR. After ELP3 and ALKBH8 silencing we visualize a downregulation in mRNA levels of these genes and no differences in the other conditions at independently experiments. Standard deviations were also calculated, based on the Ct standard deviation of the three technical replicates and converted to fold change. Unpaired-t test was used. $P < .001$ was considered highly significant (***), and $P < .05$ (**) was considered significant ($N = 3$).

i. tRNA modifying enzyme fluorescent based siRNA screen

After validating the transfection conditions, fluorescence microscopy analysis of transfected cells with the siCTRL, siELP3 and siALKBH8 were performed to identify if any of the tested enzymes interfered with proteostasis. Our results indicated that Knockdown of ELP3 led to the re-localization of HSP27-GFP to *foci* (arrows) when compared with the control condition, and in formation of only discrete green *foci* (arrows) after knockdown of ALKBH8 (Figure 15).

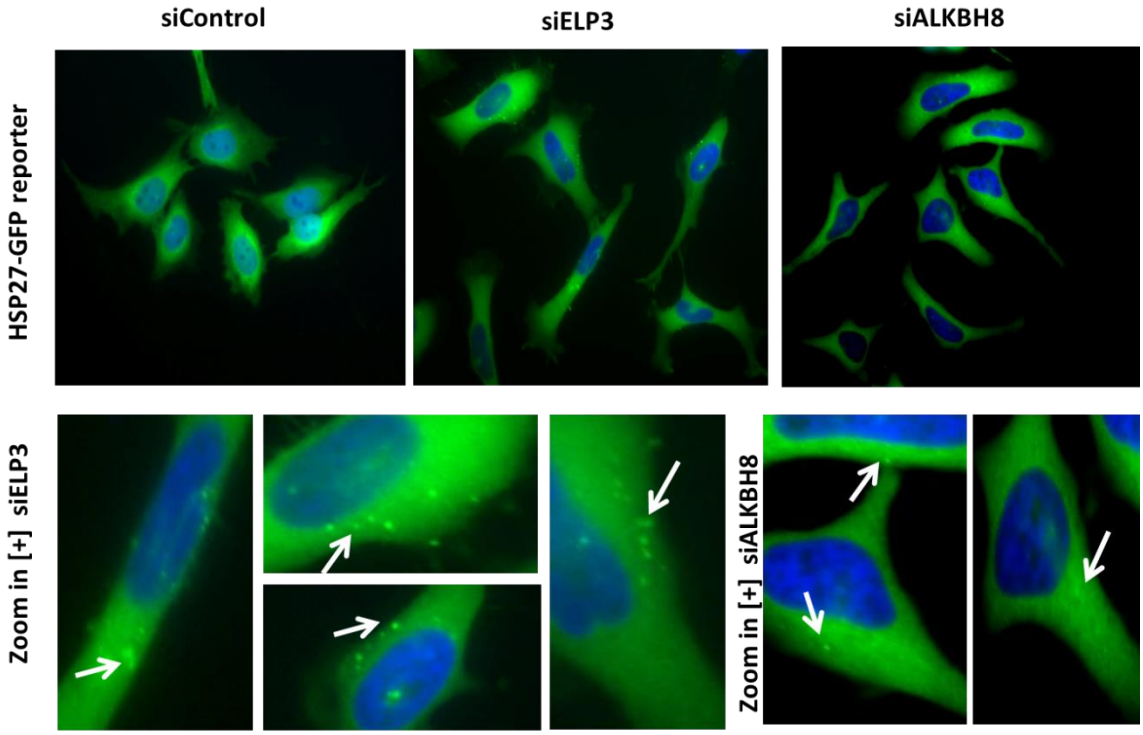

Figure 15: Fluorescent images of HeLa HSP27-GFP cell line after transfection with a siCTRL, siELP3 and siALKBH8; cell *nuclei* (blue). The presence of fluorescent *foci* are clearly visible and indicated by arrows after ELP3 knockdown, when compared to the control condition. Silencing of ALKBH8 led to accumulation of discrete fluorescent foci and only in a minority of the transfected cells. Images obtained by Zeiss Axio Imager Z1 automated microscope, magnification 60x.

A recent finding describes ALKBH8 as a central regulators of cellular oxidative stress responses in mammalian systems. Using a new gene targeted knockout mouse cell system researchers have shown that ALKBH8-/- embryonic fibroblasts (MEFs) display elevated Reactive Oxygen Species (ROS) levels, increased DNA and lipid damage – hallmarks of cellular stress (104). Furthermore, treatment of those cells with various DNA damaging agents led to a pronounced increased sensitivity of ALKBH8-/- MEFs, relative to wild type, to H_2O_2 and Rotenone – which are both known to increase intracellular ROS, with Rotenone being an endogenous ROS inducer through its ability to perturb mitochondrial function (104). Knowing this, we investigated

phenotype alterations in mitochondria's, in cells transfected with siALKBH8 and siELP3, using the MitoTracker® Red CM-H2XRos Kit.

In control cells, mitochondria are uniformly distributed throughout the cytoplasm showing the typical elongated shape. After ELP3 knockdown no significant alterations in mitochondrial arquitecture was found. However, after the treatment with siALKBH8, mitochondria are fragmented, forming packed masses in the cytoplasm (Figure 16), which are typical features of apoptosis (103,104).

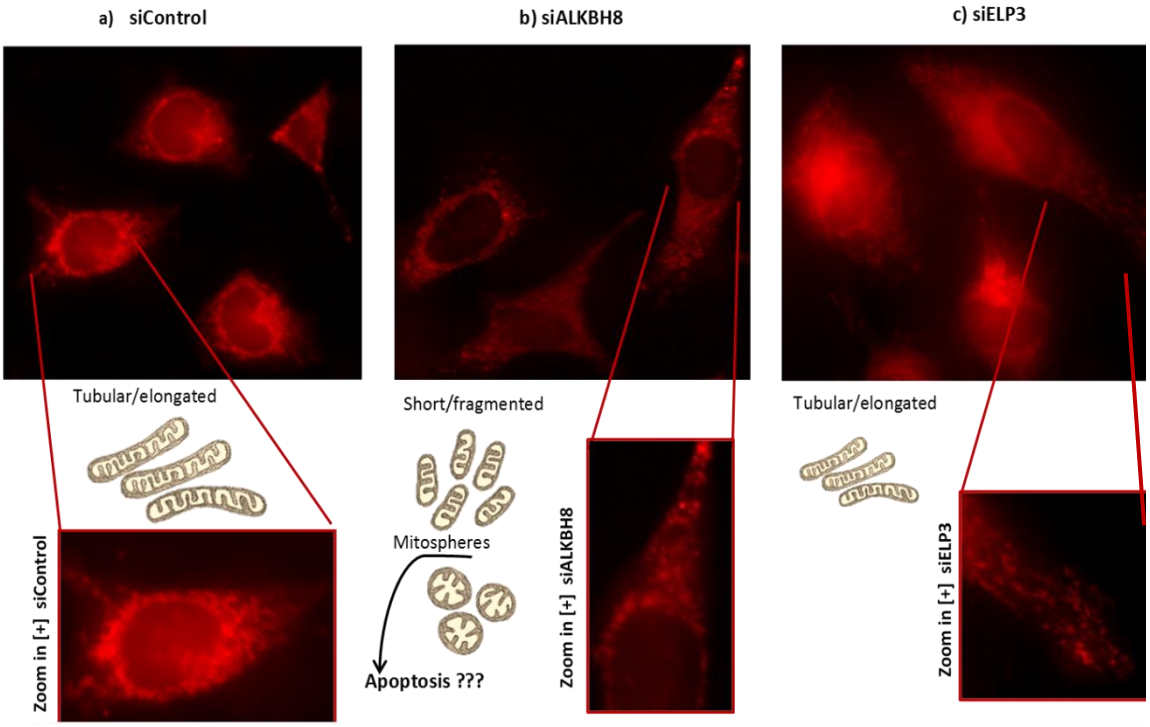

Figure 16: Morphological features of mitochondria: a) control cells b) cells treated with siALKBH8 and c) Cells treated with siELP3. Note in a), c) the presence of elongated mitochondria's and in case b) its fragmentation (with spherically-shaped – mitospheres), which were previously linked to a decrease in mitochondrial activity and may result in cellular apoptosis.

Insoluble proteins were observed 72 hours after reverse transfection with the siRNAs. Total protein was extracted and quantified with subsequent extraction of the insoluble fraction which was run by SDS-PAGE and observed on the Odyssey IR scanner. An increase in insoluble protein fraction in ELP3 knockdown cells was observed, which was in accordance with the accumulation of fluorescent foci observed by fluorescent microscopy (Figure 17).

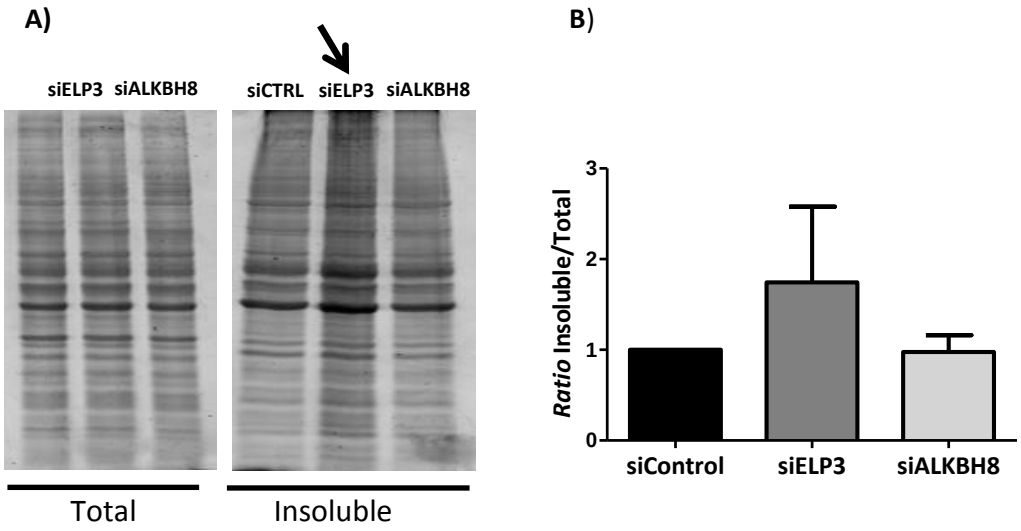

Figure 17: Analysis of the insoluble fraction of transfected cells. A) SDS-PAGE of total and insoluble protein fractions for each transfection condition. The insoluble profile of cells transfected with siELP3 is more pronounced than the other profiles, indicating an accumulation of insoluble proteins. B) Relative amount of insoluble fraction protein in transfected cells compared with the control condition (siControl). An increase in insoluble fraction in siELP3 knockdown cells is observed, but not in siALKBH8 knockdown cells. (Data analysis was done using Student's t-test (N = 3)).

Since there was an accumulation of insoluble proteins after ELP3 knockdown, we decided to analyze protein synthesis rate, as there are evidences in conformational disorders showing that increased protein aggregation is accompanied by alterations in protein synthesis (105). For that we used the Surface Sensing of Translation (SUnSET) method (106). It is based on the incorporation of puromycin, an analog of aminoacyl tRNAs, into nascent polypeptide chains, inhibiting its elongation. The nascent polypeptide can be detected with fluorescence-activated cell sorting (FACS) (Figure 18). Thus, puromycin incorporation directly infers about *in vitro* translation rate. Our preliminary data indicate that there was a decrease in puromycin incorporation in ELP3 knockdown cells, which is an indicator of a decreased protein synthesis rate. On the other hand, silencing of ALKBH8 led to a slight increase in puromycin incorporation which may indicate an increased protein synthesis rate, but further replicates are needed.

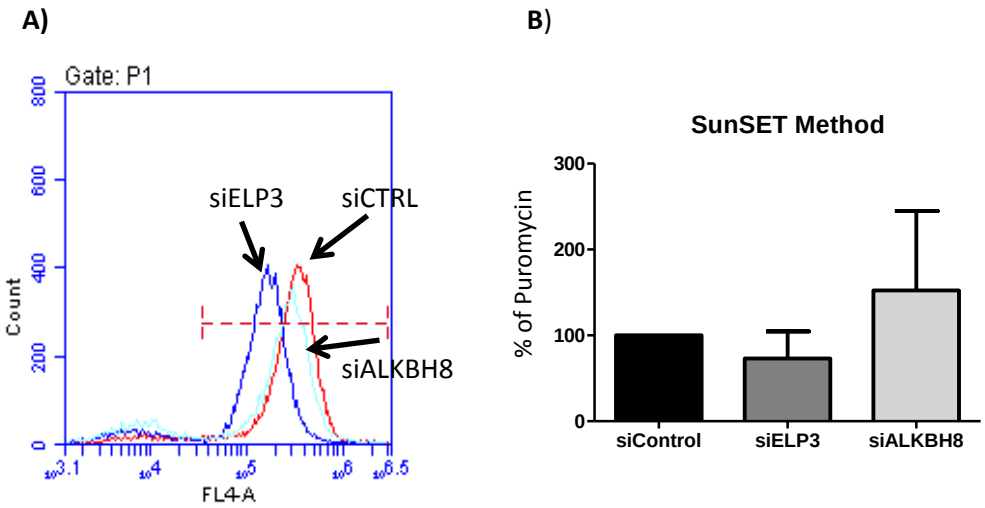

Figure 18: Fluorescence microscopy experiments were complemented with the SUnSET method to evaluate if protein synthesis rate was affected by knockdown of tRNA modifying enzymes. A) Translation analysis using puromycin-labeled proteins. B) The present graph was performed by the values obtained in the red channel of incorporated puromycin. (Still, additional replicates are needed) (N = 2)). This puromycin-based technology allow to monitor translation by FACs in individual or cell populations for siELP3 and siALKBH8 (Fluorescence was detected in the green (FL1- GFP, 510–540 nm) and red (FL4-puromycin, 660–690 nm) channels).

ii. Proteotoxic stress and quality control pathways analysis

Proteotoxic stress and quality control pathways alterations were evaluated in this study by assessing, specific components of the, UPR and UPP systems through Western blotting.

Unfolded Protein Response (UPR)

BiP is a major endoplasmic reticulum (ER) chaperone protein target of the ER stress response, or UPR, and an essential regulator of the UPR pathway. During ER stress, BiP dissociates from the three transducers (IRE1, PERK, and ATF6), effectively activating their respective UPR pathways. By Western Blot we performed the detection and quantification of BiP protein expression. The results obtained indicated a significantly decreased in BiP expression after knockdown of ALKBH8 comparison to the control (Figure 19).

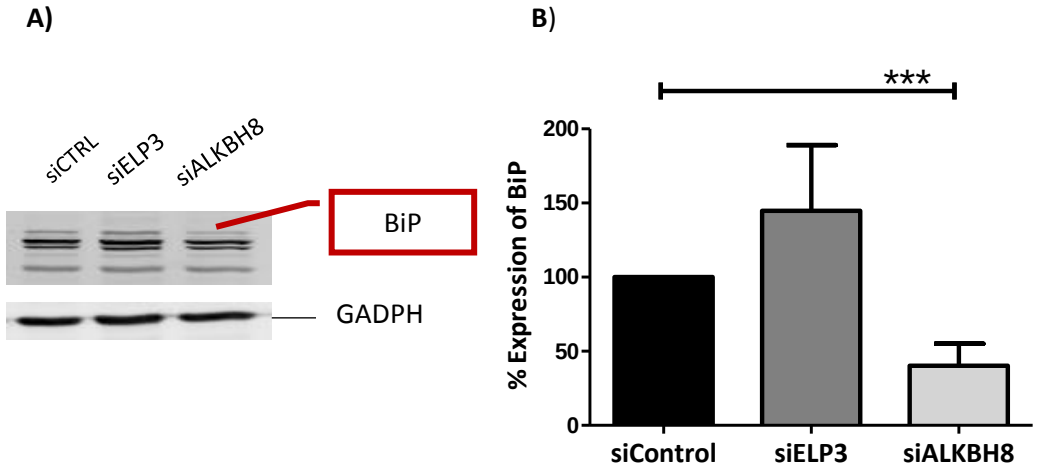

Figure 19: Analysis of BiP expression. A) The respective bands of western blot; B) Graphic of the percentage of the BiP factor in HeLa HSP27-GFP cells; no statistically significant changes were observed in siELP3 knockdown cells; statistically significant changes were observed in siALKBH8 knockdown cells, where BiP expression was downregulated; (Data analysis was done using Student's t-test; $p < .001$ was considered highly significant (***) (N = 7)).

When the cell is experiencing proteotoxic stress, the ATF6 factor is cleaved. The resultant fraction induces the transcription of chaperones and enzymes responsible for protein folding by helping the cell surviving to proteotoxicity. An expression of ATF6 cleaved increases, moderately, in siELP3 when compared to siControl transfected cells (Figure 20).

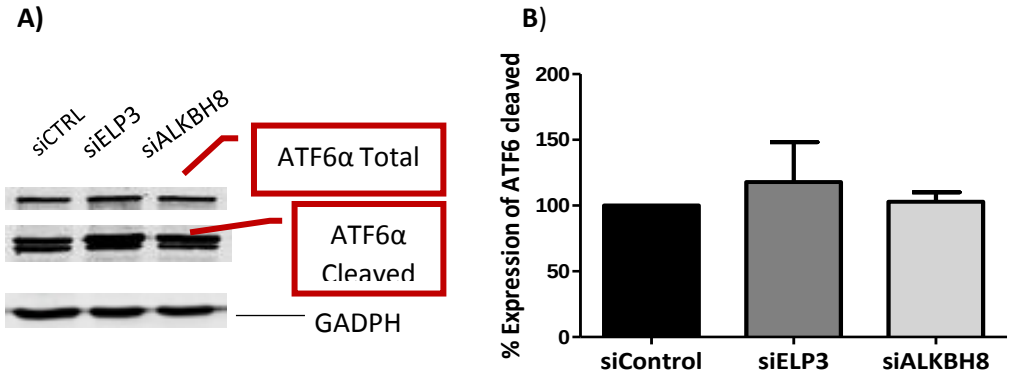

Figure 20: Analysis of ATF6 factor expression. A) The respective western blot bands are depicted; B) Graphic of percentage of the ATF6 factor cleaved in HeLa cells with Hsp27-GFP reporter. No statistically significant changes were observed relative to the control; (Data analysis was done using Student's t-test (N = 4)).

The eIF2α is a translation initiation factor which, when phosphorylated, inhibits protein synthesis. The expression of eIF2α-P factor did not change in any of the tested condition relative to the control (Figure 21).

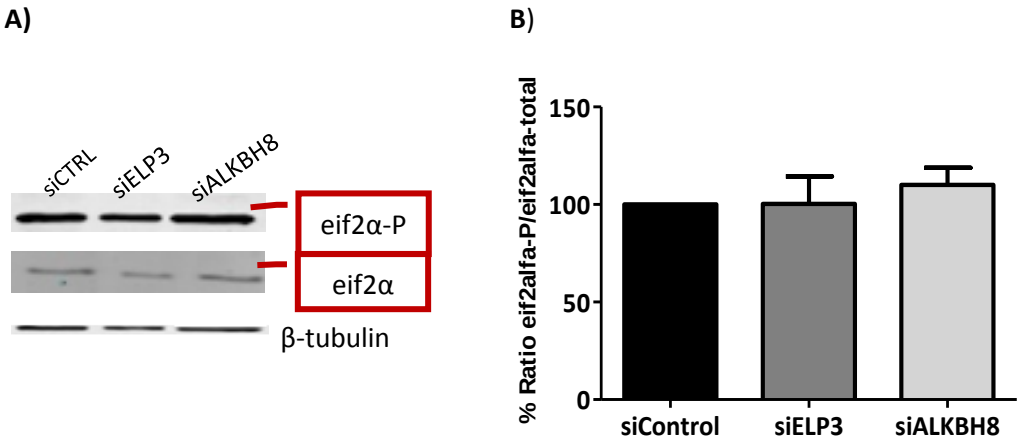

Figure 21: Analysis of eIF2α and eIF2α-P expression. A) The respective western blot bands, eif2α, eif2α-P and the endogenous control - β-tubulin are depicted; B) Graphic of % of *ratio* between eif2α-P and eif2α-Total, in HeLa HSP27-GFP cells. No statistically significant changes were observed relative to the control; (Data analysis was done using Student's t-test (N = 6)).

Ubiquitin-Proteasome Pathway Activation (UPP)

Ubiquitin is a protein that recognizes misfolding proteins and binds to them for proteasome degradation. Before substrate degradation the ubiquitin molecules are released and recycled. The anti-ubiquitin antibody labels several ubiquitinated proteins in the total extract profile. After quantification and normalization, we observed an increase in siELP3 ubiquitination relative to the control (Figure 22).

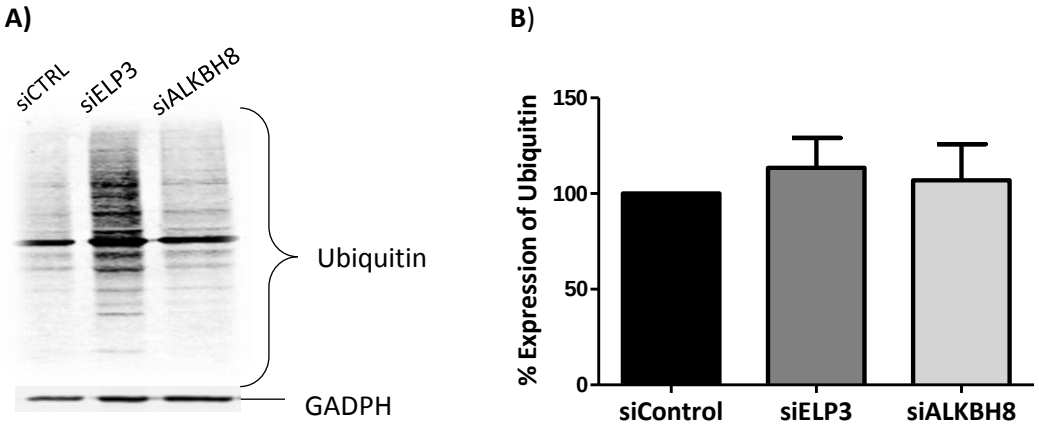

Figure 22: Analysis of protein ubiquitination. A) The respective western blot bands are depicted; B) Graphic of the percentage of ubiquitin expression in HeLa HSP27-GFP cells. No statistically significant changes were observed concerning to the control and the siELP3 condition and concerning to the control and the condition of siALKBH8, however, cells transfected with siELP3 have higher amounts of ubiquitin than the other conditions; (Data analysis was done using Student's t-test (N = 3)).

Ongoing work: After we performed all the reported experiments and established the best conditions to perform the siRNA screen, we expanded our screening and started to test the implication in proteostasis of other tRNA modifying enzymes. Thus, we obtained the fluorescent microscopy images for the elongator complex members (ELP1-ELP6) (Figures 23) and for other tRNA modifying enzymes that catalyze modifications at the position 34, such as, CTU1, IKBKAP, NSUN2, FSTJ1 and QTRT1. Not all the tRNA modifying enzymes studied lead to re-localization of our reporter (Figure 24). However, additional experiments need to be performed to draw a final conclusion concerning which of these enzymes are involved in protein aggregate accumulation.

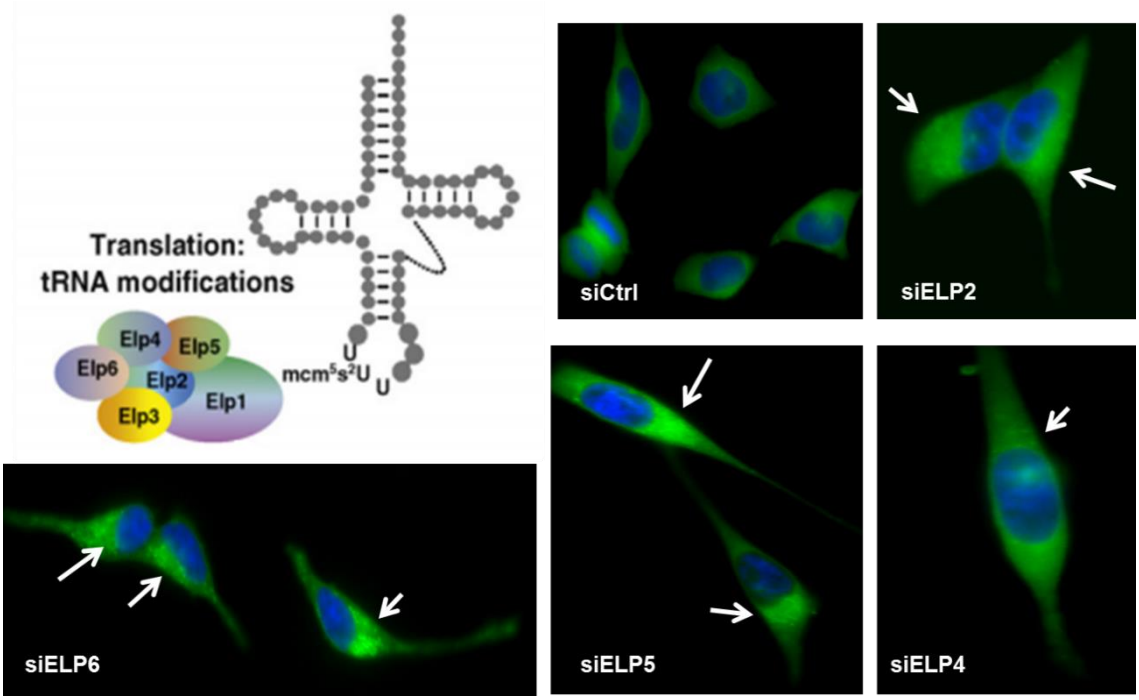

Figure 23: Fluorescent images of HeLa HSP27-GFP cell line after transfection with si(ELP2-ELP6 without ELP3). The presence of fluorescent *foci* are indicated by arrows. Images obtained by Zeiss Axio Imager Z1 automated microscope, magnification 60x. Green – GFP, Blue – Hoescht, n=1.

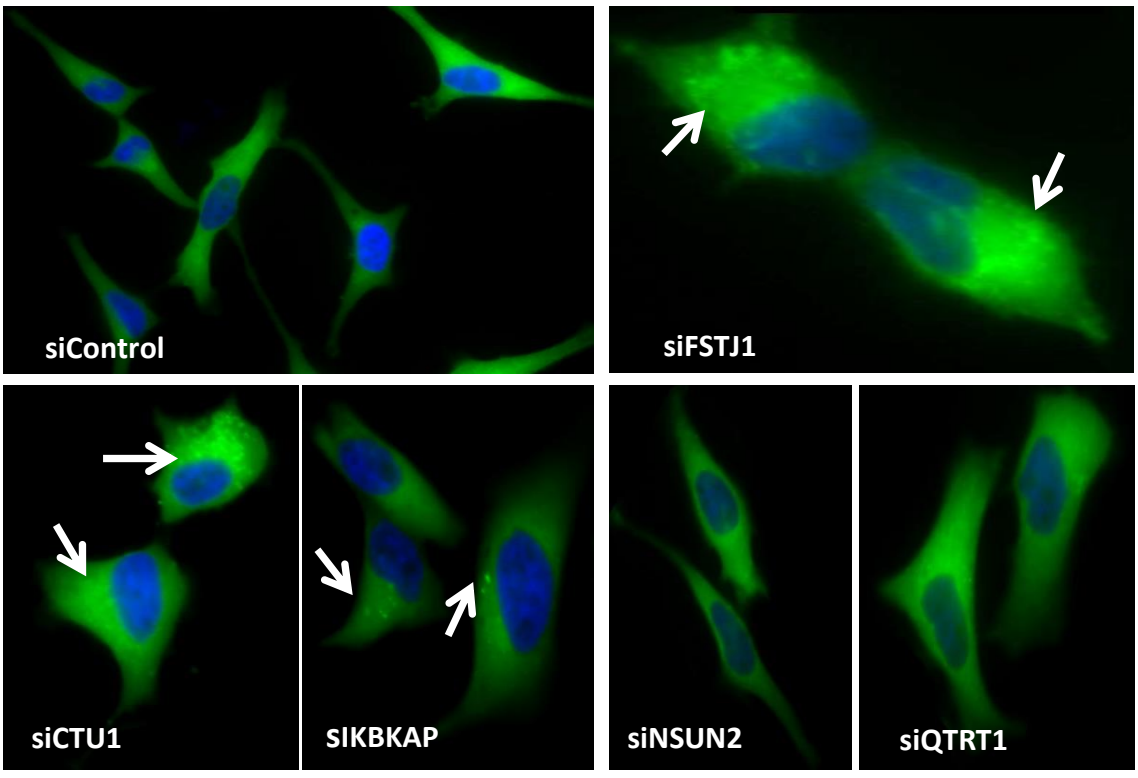

Figure 24: Evaluation of protein aggregation by fluorescence microscopy after knockdown of some tRNA modifying enzymes at position 34. Not all tRNA modifying enzymes lead to re-localization of HSP27-GFP to *foci* (arrows) when compared with the control. Further experiments are ongoing. Images obtained by Zeiss Axio Imager Z1 automated microscope, magnification 60x. Green – GFP, Blue – Hoescht, n=1.

CHAPTER 4.

Discussion

4.1. Evaluation and optimization of the HSP27-GFP sensor expressed in the stable cell line

HSP27 plays important roles in cells. This chaperone is involved in protein folding, oxidative stress reduction, suppression of apoptosis pathways and regulation of cytoskeletal actin in cancer, neurodegenerative and cardiovascular diseases (107,108). HSP27 is constitutively expressed in most human cells, but its expression levels increase in many types of cancer cells making HSP27 an attractive therapeutic target (109). As expected, in the fluorescent images we observed that unstressed cells displayed a homogeneous HSP27-GFP expression and no aggregation (Figure 10).

To evaluate the efficiency of our sensor, we used incubated cells with MG132, a peptide aldehyde inhibitor of the proteolytic activity of the 26S proteasome complex. It has been reported that proteasome inhibitors block the degradation of abnormal proteins, leading to their accumulation and activation of the UPR response and synthesis of heat shock proteins, in particular HSP27 (110,111). Our western blotting results confirm an increase in HSP27 expression, after treatment with MG132 (Figure 12), that was accompanied by an increased expression of the HSP27-GFP fusion and a re-localization of GFP fluorescence to *foci*, observed by fluorescence microscopy indicating that protein misfolding was increased and HSP27 was being recruited to refold those proteins (Figure 10).

An alternative approach to understand the contribution of the UPP machinery in detection of aggregated proteins inside aggresomes and inclusion bodies has been explored by ProteoStat® Aggresome Detection Kit (96). To evaluate the functionality of our reporter we verified the fluorescence co-localization with this commercial kit. The preliminary results indicated that our reporter is capable of detecting not only misfolding proteins but also aggregated proteins (Figure 10). In addition, we observed an accumulation of particular insoluble proteins in the insoluble fraction of cells exposed to MG132 and not in control cells, corroborating the fluorescence data (Figure 11).

Taken together, these results validated our stable cell line expressing the sensor as adequate to identify, by fluorescence microscopy, situations where protein misfolding is occurring. Thus, this stable cell line expressing the fusion sensor HSP27-GFP is a good candidate to perform siRNA fluorescence based screens to identify genes that are associated with protein aggregation. This reporter offers advantages over other protein-aggregation reporters as it is able to detect general protein aggregation, while others can only detect aggregation of a specific type of protein (98,99,112). For example, a recently developed reporter to monitor protein aggregation uses a split *Gaussia* luciferase reporter fused to Aβ40/42 that allows the

monitorization of Aβ oligomer formation, a key process in Alzheimer´s pathogenesis (98). A luciferase-based protein aggregate reporter allows assessing the poly(Q) aggregation found in Huntington disease. This reporter directly assesses protein aggregation by means of luciferase activity loss (99). Finally, the first report that directly correlates the average cellular fluorescence intensity to the extent of misfolding/aggregation of a target protein, in mammalian cells, was reported to use GFP as a folding reporter fused to the C-terminus of a panel of human copper/zinc SOD1 mutants. The major aim of this method is to understand the aggregation process of SOD1 variants and the identification of their inhibitors (112). Since our fluorescent sensor is based on the recruitment of HSP27 to misfolded proteins, it is able to recognize any protein misfolding situation that implies HSP27 recruitment, and consequently it is not restricted to the identification of a particular protein family.

4.2. ELP3 knockdown affects proteostasis

Several studies indicate that post-transcriptional nucleoside modifications of tRNAs at the anticodon wobble U_{34} are highly conserved (12,113,114) . We analyzed some enzymes that catalyze chemical modifications at the above-mentioned position, including the ELP3 and ALKBH8 enzymes. More specifically, how the knockdown of these modifications affects proteostasis. The results obtained by MTT and RT-PCR assays indicated a successful knockdown of both enzymes with the respective siRNAs, with low levels of cytotoxicity of the transfection agent and an efficient silencing of both ELP3 and ALKBH8 (Figures 13 and Figure 14).

Previous studies have shown that knockdown of ELP3 in zebrafish embryos resulted in dose-dependent motor axonal abnormalities which is, in fact, a determinant factor in ALS disorder (35). ALS is a neurodegenerative disease characterized by axonal retraction that results in denervation of the lower motor neurons, muscle dysfunction and consequent atrophy (115). The majority of ALS cases are considered to be protein misfolding disorders as the mutations found in specific genes (specially, missense mutations in SOD1 gene (chromosome 21)), cause the accumulation of misfolded proteins and their aggregation in the cell bodies and axons (115). Current findings indicate that these aggregates or, more likely, their oligomeric complex precursors, disturbe normal protein homeostasis and induce cellular stress (116). Moreover, evidences show that allelic variants of ELP3 are associated with ALS in humans. Indeed, a post-mortem study correlates the low levels of ELP3 expression in ALS individuals' brains with a genotype variation of this gene. Also, a genetic screen in *Drosophila* identified two different loss of function mutations, both in ELP3 in neuronal communication – synaptic defects – and survival

– aberrant axonal outgrowth (35). As ELP3 knockdown led to accumulation of protein aggregates, as shown in this thesis, and, as it is known, this enzyme is involved in ALS development, it is reasonable to speculate that lack of ELP3 activity in ALS is correlated with the proteostasis impairments characteristic of this disease. Our results clearly show that knockdown of ELP3 and other Elongator components induces the re-localization of HSP27-GFP to *foci* when compared with the control (Figure 15). As the reporter used detects protein aggregation, we can assume that when re-localization of green *foci* occurs, misfolding proteins are increased, which is in accordance with the findings by other group regarding the proteostasis impairment in the absence of ELP3 or U_{34} modifications. In yeast, a functional Elongator complex is crucial for the translation of stress-related genes. Yeast lacking ELP3, for example, had an impaired response to stress conditions as they cannot translate specific stress-induced mRNAs as efficiently as the wild type cells that have the required modification that allows a more efficient codon recognition (117). Also, a recent study shows that lack of U_{34} both in *S. cerevisiae* and *C. elegans* leads to translation inefficiency and proteotoxic stress (26). Although this study did not focus on ELP3, it shows the impact of the lack of modifications in position 34 in proteostasis. As ELP3 is involved in such modifications, this study indicates that defects in this enzyme (or others in particular the ones belonging to the Elongator complex) may lead to proteostasis impairments due to ribosome pausing, for example. Furthermore, it was demonstrated that deletion of ELP3 in cortical stem cells triggers ER stress and the activation of UPR response and autophagy by decreasing codon translation rates (118). Through the SUnSET method we confirmed a decrease in protein synthesis rate after ELP3 knockdown (Figure 18), but further replicas are needed to draw definitive conclusions. Additionally, results illustrated in figure 17 confirmed that an increase in the insoluble protein fraction also causes alterations in protein expression profiles. Evidences also showed that increased protein aggregation is accompanied by alterations in protein synthesis (105).

Aggregates found in ALS patients, as well as mouse models, contain ubiquitin, a protein required to target proteins *via* the proteasome degradation pathway (119). The misaccumulation of ubiquitinated misfolded proteins might badly affect the proteasome machinery and, consequently, impair normal proteasome degradation. Our results indicated a slight increase in ubiquitinated proteins in ELP3 knockdowns, indicating that the proteasome was probably being affected by the absence of this enzyme (Figure 22) in detriment of non-activation of UPR response (Figure 19, Figure 20 and Figure 21). If the load of misfolded proteins accumulated in cells, due to ELP3 absence, exceeds the cell ability to cope with them, we expect that the proteasome is negatively affected and its activity is decreased. The hypothesis that aberrations in the ubiquitin/proteasome system may contribute to human disorders

characterized by accumulation of misfolded proteins has been supported (116,120,121). These studies indicate that the continued expression of mutant SOD1 leads to proteasome inhibition and motor neuronal death, which in part explains the pathogenesis of mutant SOD1-linked ALS (121). Also, a transient expression of aggregated poly(Q) proteins cause inhibition of the UPP (120,122). These findings postulate that protein aggregates can inhibit the UPP by saturating the capacity of one or more molecular chaperones required for UPP function or by direct interaction with the proteasome catalytic subunits (123,124), which is in accordance with our data.

As mentioned, we performed a preliminary screening including other tRNA modifying enzymes. Knockdown of most of the ones belonging to the Elongator Complex resulted in accumulation of misfolded proteins in the cell cytoplasm (Figure 23). As previously mentioned, several studies associated some ELP3 variants with ALS, strongly suggesting that the Elongator-dependent pathways may be deregulated in distinct neurological disorders (101). Evidences showed that the subunit 4 depletion results in the brain-specific downregulation of genes implicated in cell motility and migration**,** whereas a study identified ELP5 and ELP6 as key players for migration, invasion and tumorigenicity of melanoma cells, as integral subunits of Elongator (102, 103). Taken together, this data points out for a relevant role of different elongator complex members in different cellular mechanisms indicating that deregulation of these enzymes will have an impact in the cell's function. However, additional experiments are needed to unequivocally conclude the relevance of those enzymes for proteostasis and whether their mechanism is similar to ELP3, or not.

4.3. ALKBH8 knockdown does not induce protein misfolding but affects mitochondria

We only found discrete green *foci* in cells, when ALKBH8 was silenced (Figure 15), indicating that knockdown of this enzyme was not affecting proteostasis in a significant manner. However, ALKBH8 -/- mice display an extensive mismodification of wobble uridines that reduced the fidelity and efficiency of protein translation by recoding of the UGA stop codon to Selenocysteine (Sec) (125).

Recent evidences showed that knockdown of ALKBH8 enzyme induces apoptosis in bladder cancer cells *via* downregulating the protein expression of survivin (126). We also observed an increase in cell death after ALKBH8 knockdown, but we still need to perform additional experiments to verify if apoptosis is, in fact, increasing in the absence of ALKBH8. In addition, survivin is also reported in tumorigenesis through the interaction with caspase 3 and 7 and inhibition of Bax and Fas induced apoptosis (127,128). These studies pointed to a possible

correlation between apoptosis activation and an alteration in mitochondrial morphology and, in fact we observed that after this enzyme knockdown, mitochondria were severely affected and most of them were fragmented forming packed masses in the cytoplasm (Figure 16).

Notably, we found that BiP was downregulated upon ALKBH8 knockdown (Figure 19), but this phenomenon was not accompanied by deregulation of other UPR-related proteins. Nevertheless, a study indicates that higher levels of BiP would delay or prevent UPR, whereas lower levels could cause a premature or prolonged UPR (129). Further studies are required to understand the role of ALKBH8.

4.4. Conclusions and future work

The knowledge on the roles that tRNA modifying enzymes play in human diseases is opening a whole new and exciting field for research and for development of novel therapeutics. The vast majority of the published research on tRNA modifications has been carried out in bacteria, in lower eukaryotes and, to less extent, in mammalian cell lines.

Our major goal was the implementation of a tRNA modifying enzyme fluorescent based siRNA screen using a stable cell line expressing a protein aggregation reporter system – HSP27-GFP. The evaluation of our reporter indicated that it can be a good candidate in siRNA fluorescence based screens to identify genes associated with protein aggregation. Fluorescence microscopy experiments revealed that Knockdown of ELP3 resulted in re-localization of HSP27-GFP to *foci*. This situation was less evident after ALKBH8 silencing. The mitochondrial morphology was also evaluated. We found more fragmented mitochondrias in the cytoplasm of siALKBH8 cells, indicating a possible dysfunction. In the case of siELP3, the fluorescent data were complemented with an increase of the insoluble protein fraction and a decrease in protein synthesis *rate*. The activation of UPR and UPP were also studied by western blotting, but further replicates are needed to draw definitive conclusions on the activation of the UPR. All findings indicated that downregulation of ELP3 affects protein folding and proteostasis and, in case of ALKBH8, some protein misfolding may be occurring, but is possible that the main consequence of ALKBH8 downregulation is apoptosis induction. Additional screening of others tRNA modifying enzymes that catalyze modifications at the position 34 are ongoing.

The results obtained expanded our knowledge about the biological function of tRNA modifying enzymes, in particular its impact in proteostasis. In a near future, the presence of apoptotic cell populations will be analyzed by flow cytometry, through Annexin V, and the proteins in the insoluble protein fraction of ELP3 knockdown cells will be identified by mass spectrometry. To identify genes and other signaling pathways that may be deregulated due to absence of tRNA modifying enzymes, we will perform gene expression microarrays. We also intend to study the effects of upregulation in some tRNA modifying enzymes.

This research contributed to the establishment of a stable cell line expressing a protein aggregation fluorescent sensor that can be used to perform genetic screenings as well as screenings of chemical compounds. Moreover, by using this stable cell line expressing the developed fluorescent sensor, we were able to identify ELP3 as a relevant enzyme for proteostasis and further studies are ongoing to validate this molecule as a novel therapeutic target for age-related diseases.

We believe that in the near future other tRNA modifying enzymes will be identified as proteostasis regulators thanks to the implementation of our siRNA screening.

Acknowledgements:

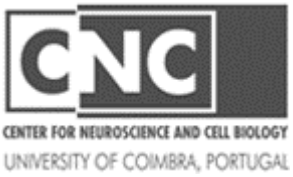

References

1. “Francis Crick - Biographical”. Nobelprize.org. Nobel Media AB 2014. Web. 9 Aug 2016. [Internet]. The Nobel Foundation 1962. 2014. Available from: http://www.nobelprize.org/nobel_prizes/medicine/laureates/1962/crick-bio.html.
2. Watson JD, Crick FHC. Molecular structure of nucleic acids [Internet]. Nature. 1953. p. 737–8. Available from: http://www.nature.com/physics/looking-back/crick/%5Cnhttp://www.ncbi.nlm.nih.gov/pubmed/13054692.
3. Alberts B, Johnson A, Lewis J et al. From RNA to Protein. In: Molecular Biology of the Cell [Internet]. 4th editio. New York: Garland Science; 2002. Available from: http://www.ncbi.nlm.nih.gov/books/NBK26829/.
4. Crick F. On degenerate templates and the adaptor hypothesis: A note for the RNA tie club. Orig Repos Wellcome Libr Hist Underst Med [Internet]. 1955;18. Available from: http://archives.wellcome.ac.uk/.
5. Crick FH. The genetic code--yesterday, today, and tomorrow. Cold Spring Harb Symp Quant Biol. 1966;31:1–9.
6. Lobanov A V, Turanov AA, Hatfield DL, Gladyshev VN. Dual functions of codons in the genetic code. Crit Rev Biochem Mol Biol [Internet]. 2010;45(4):257–65. Available from: http://www.pubmedcentral.nih.gov/articlerender.fcgi?artid=3311535&tool=pmcentrez&rendertype=abstract.
7. GM. C. Protein Synthesis, Processing, and Regulation. In: The Cell: A Molecular Approach [Internet]. 2nd editio. Sunderland (MA): Sinauer Associates; 2000. p. 310–50. Available from: http://www.ncbi.nlm.nih.gov/books/NBK9849/.
8. Allan Drummond D, Wilke CO. The evolutionary consequences of erroneous protein synthesis. Nat Rev Genet [Internet]. Nature Publishing Group; 2009;10(10):715–24. Available from: http://www.nature.com/doifinder/10.1038/nrg2662.
9. Marintchev A, Wagner G. Translation initiation: structures, mechanisms and evolution. Q Rev Biophys [Internet]. 2004;37(3–4):197–284. Available from: papers://945a2e4a-ca32-4571-b6af-fe1327b27ce1/Paper/p2082.
10. Dever TE, Green R. Phases of Translation in Eukaryotes. 2015;1–16.
11. Jackson RJ, Hellen CUT, Pestova T V. The mechanism of eukaryotic translation initiation and principles of its regulation. Nat Rev Mol Cell Biol [Internet]. Nature Publishing Group; 2010;11(2):113–27. Available from: http://www.nature.com/doifinder/10.1038/nrm2838.
12. Schaffrath R, Leidel SA. Wobble uridine modifications – a reason to live, a reason to die?! RNA Biol [Internet]. Taylor & Francis; 2017;0(0):0–0. Available from: https://www.tandfonline.com/doi/full/10.1080/15476286.2017.1295204.
13. Crick FH. Codon--anticodon pairing: the wobble hypothesis. J Mol Biol. 1966;19(2):548–55.

14. Agris PF, Vendeix FAP, Graham WD. tRNA's Wobble Decoding of the Genome: 40 Years of Modification. J Mol Biol. 2007;366(1):1–13.
15. Fernández-Millán P, Schelcher C, Chihade J, Masquida B, Giegé P, Sauter C. Transfer RNA: From pioneering crystallographic studies to contemporary tRNA biology. Arch Biochem Biophys [Internet]. Elsevier Ltd; 2015; Available from: http://dx.doi.org/10.1016/j.abb.2016.03.005.
16. Tuorto F, Lyko F. Genome recoding by tRNA modifications. Open Biol [Internet]. 2016;6(12):160287. Available from: http://dx.doi.org/10.1098/rsob.160287%0Ahttp://rsob.royalsocietypublishing.org/lookup/doi/10.1098/rsob.160287.
17. Rich A, Kim SH. The Three-dimensional Structure of Transfer RNA of its structure has clarified the mechanism of protein synthesis. 1977;52–63.
18. Agris PF. Wobble position modified nucleosides evolved to select transfer RNA codon recognition: A modified-wobble hypothesis. Biochimie. 1991;73(11):1345–9.
19. Wilusz JE. Controlling translation via modulation of tRNA levels. Wiley Interdiscip Rev RNA. 2015;6(4):453–70.
20. Shigematsu M, Honda S, Kirino Y. Transfer RNA as a source of small functional RNA. J Mol Biol Mol imaging [Internet]. 2014;1(2):1–15. Available from: http://www.pubmedcentral.nih.gov/articlerender.fcgi?artid=4572697&tool=pmcentrez&rendertype=abstract.
21. Park SG, Schimmel P, Kim S. Aminoacyl tRNA synthetases and their connections to disease. Proc Natl Acad Sci U S A [Internet]. 2008;105(32):11043–9. Available from: http://europepmc.org/articles/PMC2516211/?report=abstract.
22. Ribas de Pouplana L, Schimmel P. Two classes of tRNA synthetases suggested by sterically compatible dockings on tRNA acceptor stem. Cell. 2001;104(2):191–3.
23. Antonellis A, Green ED. The role of aminoacyl-tRNA synthetases in genetic diseases. Annu Rev Genomics Hum Genet. 2008;9:87–107.
24. Björk GR, Ericson JU, Gustafsson CED, Hagervall TG, Jönsson YH, Wikström RM. Transfer RNA modification. Annu Rev Biochem [Internet]. 1987;56:263–87. Available from: http://www.ncbi.nlm.nih.gov/pubmed/12154398.
25. Grosjean H, de Crécy-Lagard V, Marck C. Deciphering synonymous codons in the three domains of life: Co-evolution with specific tRNA modification enzymes. FEBS Lett [Internet]. Federation of European Biochemical Societies; 2010;584(2):252–64. Available from: http://dx.doi.org/10.1016/j.febslet.2009.11.052.
26. Nedialkova DD, Leidel SA. Optimization of Codon Translation Rates via tRNA Modifications Maintains Proteome Integrity. Cell [Internet]. The Authors; 2015;161(7):1606–18. Available from: http://dx.doi.org/10.1016/j.cell.2015.05.022.
27. Manuscript A, Nanostructures SPC. Transfer RNA modifications: Nature's combinatorial chemistry playground Jane. Nano. 2008;6(9):2166–71.

28. Deng W, Babu IR, Su D, Yin S, Begley TJ, Dedon PC. Trm9-Catalyzed tRNA Modifications Regulate Global Protein Expression by Codon-Biased Translation. PLoS Genet. 2015;11(12):1–23.
29. Klassen R, Ciftci A, Funk J, Bruch A, Butter F, Schaffrath R. TRNA anticodon loop modifications ensure protein homeostasis and cell morphogenesis in yeast. Nucleic Acids Res. 2016;44(22):10946–59.
30. Torres AG, Piñeyro D, Filonava L, Stracker TH, Batlle E, Ribas De Pouplana L. A-to-I editing on tRNAs: Biochemical, biological and evolutionary implications. FEBS Lett [Internet]. Federation of European Biochemical Societies; 2014;588(23):4279–86. Available from: http://dx.doi.org/10.1016/j.febslet.2014.09.025.
31. Alazami AM, Hijazi H, Al-Dosari MS, Shaheen R, Hashem A, Aldahmesh M a, et al. Mutation in ADAT3, encoding adenosine deaminase acting on transfer RNA, causes intellectual disability and strabismus. J Med Genet [Internet]. 2013;50(7):425–30. Available from: http://www.ncbi.nlm.nih.gov/pubmed/23620220.
32. Guy MP, Shaw M, Weiner CL, Hobson L, Stark Z, Rose K, et al. Defects in tRNA Anticodon Loop 2'-O-Methylation Are Implicated in Nonsyndromic X-Linked Intellectual Disability due to Mutations in FTSJ1. Hum Mutat. 2015;36(12):1176–87.
33. El-Hattab AW, Bournat J, Eng PA, Wu JBS, Walker BA, Stankiewicz P, et al. Microduplication of Xp11.23p11.3 with effects on cognition, behavior, and craniofacial development. Clin Genet. 2011;79(6):531–8.
34. Dai L, Xing L, Gong P, Zhang K, Gao X, Zheng Z, et al. Positive association of the FTSJ1 gene polymorphisms with nonsyndromic X-linked mental retardation in young Chinese male subjects. J Hum Genet. 2008;53(7):592–7.
35. Simpson CL, Lemmens R, Miskiewicz K, Broom WJ, Hansen VK, van Vught PWJ, et al. Variants of the elongator protein 3 (ELP3) gene are associated with motor neuron degeneration. Hum Mol Genet. 2009;18(3):472–81.
36. Strug LJ, Clarke T, Chiang T, Chien M, Baskurt Z, Li W, et al. Centrotemporal sharp wave EEG trait in rolandic epilepsy maps to Elongator Protein Complex 4 (ELP4). Eur J Hum Genet [Internet]. Nature Publishing Group; 2009;17(9):1171–81. Available from: http://www.pubmedcen.tral.nih.gov/articlerender.fcgi?artid=2729813&tool=pmcentrez&rendertype=abstract
37. Blanco S, Dietmann S, Flores J V, Hussain S, Kutter C, Humphreys P, et al. Aberrant methylation of tRNAs links cellular stress to neuro-developmental disorders. EMBO J [Internet]. 2014;33(18):1–20. Available from: http://www.ncbi.nlm.nih.gov/pubmed/25063673.
38. Martinez FJ, Lee JH, Lee JE, Blanco S, Nickerson E, Gabriel S, et al. Whole exome sequencing identifies a splicing mutation in NSUN2 as a cause of a Dubowitz-like syndrome. J Med Genet [Internet]. 2012;49(6):380–5. Available from: http://jmg.bmj.com/content/early/2012/05/11/jmedgenet-2011-100686.short.

39. Abbasi-Moheb L, Mertel S, Gonsior M, Nouri-Vahid L, Kahrizi K, Cirak S, et al. Mutations in NSUN2 cause autosomal- Recessive intellectual disability. Am J Hum Genet [Internet]. The American Society of Human Genetics; 2012;90(5):847–55. Available from: http://dx.doi.org/10.1016/j.ajhg.2012.03.021.

40. Alexandrov A, Martzen MR, Phizicky EM. Two proteins that form a complex are required for 7-methylguanosine modification of yeast tRNA. Rna. 2002;8(10):1253–66.

41. Alcina A, Fedetz M, Fernández Ó, Saiz A, Izquierdo G, Lucas M, et al. Identification of a functional variant in the KIF5A-CYP27B1-METTL1-FAM119B locus associated with multiple sclerosis. J Med Genet [Internet]. 2013;50(1):25–33. Available from: http://www.pubmedcentral.nih.gov/articlerender.fcgi?artid=3538279&tool=pmcentrez&rendertype=abstract.

42. Guan M-X, Yan Q, Li X, Bykhovskaya Y, Gallo-Teran J, Hajek P, et al. Mutation in TRMU related to transfer RNA modification modulates the phenotypic expression of the deafness-associated mitochondrial 12S ribosomal RNA mutations. Am J Hum Genet [Internet]. 2006;79(2):291–302. Available from: http://www.pubmedcentral.nih.gov/articlerender.fcgi?artid=1559489&tool=pmcentrez&rendertype=abstract.

43. Umeda N, Suzuki T, Yukawa M, Ohya Y, Shindo H, Watanabe K, et al. Mitochondria-specific RNA-modifying enzymes responsible for the biosynthesis of the wobble base in mitochondrial tRNAs: Implications for the molecular pathogenesis of human mitochondrial diseases. J Biol Chem. 2005;280(2):1613–24.

44. Torres AG, Batlle E, Ribas de Pouplana L. Role of tRNA modifications in human diseases. Trends Mol Med [Internet]. Elsevier Ltd; 2014;20(6):306–14. Available from: http://dx.doi.org/10.1016/j.molmed.2014.01.008.

45. Robert Schleif. 6 Protein Structure. In: Genetics and Molecular Biology [Internet]. second. Baltimore, Maryland; 1993. p. 149–77. Available from: http://gene.bio.jhu.edu/bm2whole.pdf.

46. Alberts B, Johnson A, Lewis J et al. The Compartmentalization of Cells. In: Molecular Biology of the Cell [Internet]. 4th editio. New York: Garland Science; 2002. Available from: http://www.ncbi.nlm.nih.gov/books/NBK26907/.

47. Ellgaard L, Helenius A. Quality control in the endoplasmic reticulum . Nat Rev cell Biol. 2003;4(3):181–91.

48. Ogen-Shtern N, Ben David T, Lederkremer GZ. Protein aggregation and ER stress. Brain Res [Internet]. Elsevier; 2016;1–9. Available from: http://dx.doi.org/10.1016/j.brainres.2016.03.044

49. Kim YE, Hipp MS, Bracher A, Hayer-Hartl M, Hartl FU. Molecular chaperone functions in protein folding and proteostasis. [Internet]. Annual review of biochemistry. 2013. 323-55 p. Available from: http://www.ncbi.nlm.nih.gov/pubmed/23746257.

50. Taylor JP. Toxic Proteins in Neurodegenerative Disease. Science (80-) [Internet]. 2002;296(5575):1991–5. Available from: http://www.sciencemag.org/cgi/doi/10.1126/science.1067122.

51. Wolozin B. Regulated protein aggregation: stress granules and neurodegeneration. Mol Neurodegener [Internet]. 2012;7(1):56. Available from: http://www.pubmedcentral.nih.gov/articlerender.fcgi?artid=3519755&tool=pmcentrez&rendertype=abstract.

52. Lin YF, Haynes CM. Metabolism and the UPRmt. Mol Cell. 2016;61(5):677–82.

53. Hipp MS, Park SH, Hartl UU. Proteostasis impairment in protein-misfolding and -aggregation diseases. Trends Cell Biol [Internet]. Elsevier Ltd; 2014;24(9):506–14. Available from: http://dx.doi.org/10.1016/j.tcb.2014.05.003.

54. Woerner AC, Frottin F, Hornburg D, Feng LR, Meissner F, Patra M, et al. Cytoplasmic protein aggregates interfere with nucleocytoplasmic transport of protein and RNA. Science (80-) [Internet]. 2016;351(6269):173–6. Available from: http://www.sciencemag.org/content/351/6269/173.abstract.

55. Schröder M, Kaufman RJ, Schr M. ER stress and the unfolded protein response. Mutat Res [Internet]. 2005;569(1–2):29–63. Available from: http://www.ncbi.nlm.nih.gov/pubmed/15603751.

56. Hetz C. The unfolded protein response: controlling cell fate decisions under ER stress and beyond. Nat Rev Mol Cell Biol [Internet]. Nature Publishing Group; 2012;13(2):89–102. Available from: http://dx.doi.org/10.1038/nrm3270%5Cnpapers2://publication/doi/10.1038/nrm3270

57. Walter P, Ron D. The Unfolded Protein Response: From stress pathway to homeostatic regulation. Science (80-). 2012;334(2011):1081–6.

58. Ellis RJ. The general concept of molecular chaperones. Philos Trans R Soc Lond B Biol Sci [Internet]. 1993;339(1289):257–61. Available from: http://rstb.royalsocietypublishing.org/cgi/doi/10.1098/rstb.1993.0023.

59. Gershenson A, Gierasch LM. Protein folding in the cell: Challenges and progress. Curr Opin Struct Biol [Internet]. Elsevier Ltd; 2011;21(1):32–41. Available from: http://dx.doi.org/10.1016/j.sbi.2010.11.001.

60. Park SH, Kukushkin Y, Gupta R, Chen T, Konagai A, Hipp MS, et al. PolyQ proteins interfere with nuclear degradation of cytosolic proteins by sequestering the Sis1p chaperone. Cell [Internet]. Elsevier Inc.; 2013;154(1):134–45. Available from: http://dx.doi.org/10.1016/j.cell.2013.06.003

61. Choe Y-J, Park S-H, Hassemer T, Körner R, Vincenz-Donnelly L, Hayer-Hartl M, et al. Failure of RQC machinery causes protein aggregation and proteotoxic stress. Nature [Internet]. Nature Publishing Group; 2016;531(7593):191–5. Available from: http://www.ncbi.nlm.nih.gov/pubmed/26934223.

62. Saibil H. Chaperone machines for protein folding, unfolding and disaggregation. Nat Rev Mol Cell Biol [Internet]. Nature Publishing Group; 2013;14(10):630–42. Available from: http://www.nature.com.gate1.inist.fr/nrm/journal/v14/n10/full/nrm3658.html%5Cnhttp://www.nature.com.gate1.inist.fr/nrm/journal/v14/n10/pdf/nrm3658.pdf.

63. Schroder M. The unfolded protein response. Mol Biotechnol [Internet]. 2007;108(51):20597–602. Available from: http://www.ncbi.nlm.nih.gov/pubmed/22235297.

64. Kapoor A, Sanyal AJ. Endoplasmic Reticulum Stress and the Unfolded Protein Response. Clin Liver Dis [Internet]. Elsevier Ltd; 2009;13(4):581–90. Available from: http://dx.doi.org/10.1016/j.cld.2009.07.004.

65. Lurlaro R, Muñoz Pinedo C. Cell death induced by endoplasmic reticulum stress. FEBS J [Internet]. 2015;n/a-n/a. Available from: http://doi.wiley.com/10.1111/febs.13598.

66. Tsuru A, Imai Y, Saito M, Kohno K. Novel mechanism of enhancing IRE1α-XBP1 signalling via the PERK-ATF4 pathway. Sci Rep [Internet]. Nature Publishing Group; 2016;6:24217. Available from: http://www.nature.com/articles/srep24217%5Cnhttp://www.ncbi.nlm.nih.gov/pubmed/27052593.

67. Harding HP, Zeng H, Zhang C, Jungries R, Chung P, Plesken H, et al. Diabetes mellitus and exocrine pancreatic dysfunction in Perk-I- mice reveals a role for translational control in survival of secretory cells. Mol Cell. 2001;7(6):1153–63.

68. Scheuner D, Song B, McEwen E, Liu C, Laybutt R, Gillespie P, et al. Translational control is required for the unfolded protein response and in vivo glucose homeostasis. Mol Cell [Internet]. 2001;7(6):1165–76. Available from: http://www.ncbi.nlm.nih.gov/pubmed/11430820.

69. Scheuner D, Vander Mierde D, Song B, Flamez D, Creemers JWM, Tsukamoto K, et al. Control of mRNA translation preserves endoplasmic reticulum function in beta cells and maintains glucose homeostasis. Nat Med. 2005;11(7):757–64.

70. Pasare C, Medzhitov R. Endoplasmic Reticulum Stress Links Obesity, Insulin Action, and Type 2 Diabetes. Science (80-). 2003;299(February):1033–6.

71. Company T. An initial phase of JNK activation inhibits cell death early in the endoplasmic reticulum stress response Max Brown. 2016;44(April).

72. Vidal RL, Figueroa A, Court FA, Thielen P, Molina C, Wirth C, et al. Targeting the UPR transcription factor XBP1 protects against Huntington's disease through the regulation of FoxO1 and autophagy. Hum Mol Genet. 2012;21(10):2245–62.

73. Tsuruo T, Naito M, Tomida a, Fujita N, Mashima T, Sakamoto H, et al. Molecular targeting therapy of cancer: drug resistance, apoptosis and survival signal. Cancer Sci [Internet]. 2003;94(1):15–21. Available from: http://www.ncbi.nlm.nih.gov/entrez/query.fcgi?cmd=Retrieve&db=PubMed&dopt=Citation&list_uids=12708468.

74. Li J, Lee AS. Stress induction of GRP78/BiP and its role in cancer. Curr Mol Med. 2006;6(1):45–54.

75. Lee AS. GRP78 induction in cancer: Therapeutic and prognostic implications. Cancer Res. 2007;67(8):3496–9.

76. Dufey E, Sepúlveda D, Rojas-Rivera D, Hetz C. Cellular mechanisms of endoplasmic reticulum stress signaling in health and disease. 1. An overview. Am J Physiol Cell Physiol [Internet]. 2014;307(7):C582-594. Available from: http://www.ncbi.nlm.nih.gov/pubmed/25143348.

77. The Royal Swedish Academy of Sciences. Ubiquitin-mediated proteolysis (Nobel Prize Chemistry 2004). R swedish Acad Sci. 2004;(October):12.

78. Clague MJ, Urbé S. Ubiquitin: Same molecule, different degradation pathways. Cell. 2010;143(5):682–5.

79. Komander D, Clague MJ, Urbé S. Breaking the chains: structure and function of the deubiquitinases. Nat Rev Mol Cell Biol [Internet]. Nature Publishing Group; 2009;10(8):550–63. Available from: http://dx.doi.org/10.1038/nrm2731.

80. Rogel MR, Jaitovich A, Ridge KM. The role of the ubiquitin proteasome pathway in keratin intermediate filament protein degradation. Proc Am Thorac Soc. 2010;7(1):71–6.

81. Rosenzweig R, Osmulski P a, Gaczynska M, Glickman MH. The central unit within the 19S regulatory particle of the proteasome. Nat Struct Mol Biol. 2008;15(6):573–80.

82. Tu Y, Chen C, Pan J, Xu J, Zhou ZG, Wang CY. The ubiquitin proteasome pathway (UPP) in the regulation of cell cycle control and DNA damage repair and its implication in tumorigenesis. Int J Clin Exp Pathol. 2012;5(8):726–38.

83. Schmidt M, Finley D. Regulation of proteasome activity in health and disease. Biochim Biophys Acta [Internet]. Elsevier B.V.; 2014;1843(1):13–25. Available from: http://www.ncbi.nlm.nih.gov/pubmed/23994620.

84. Moore DJ, Dawson VL, Dawson TM. Role for the ubiquitin-proteasome system in Parkinson's disease and other neurodegenerative brain amyloidoses. Neuromolecular Med. 2003;4(1–2):95–108.

85. Storrie B, Starr T, Forsten-williams K. Membrane Trafficking. 2008;457:179–92. Available from: http://www.springerlink.com/index/10.1007/978-1-59745-261-8.

86. Schneider JL, Cuervo AM. Autophagy and human disease: Emerging themes. Curr Opin Genet Dev [Internet]. Elsevier Ltd; 2014;26:16–23. Available from: http://dx.doi.org/10.1016/j.gde.2014.04.003.

87. Yamamoto H, Kakuta S, Watanabe TM, Kitamura A, Sekito T, Kondo-Kakuta C, et al. Atg9 vesicles are an important membrane source during early steps of autophagosome formation. J Cell Biol. 2012;198(2):219–33.

88. Yang Z, Klionsky DJ. Mammalian autophagy: Core molecular machinery and signaling regulation. Curr Opin Cell Biol [Internet]. Elsevier Ltd; 2010;22(2):124–31. Available from: http://dx.doi.org/10.1016/j.ceb.2009.11.014.

89. Lamark T, Johansen T. Aggrephagy: Selective disposal of protein aggregates by macroautophagy. Int J Cell Biol. 2012;2012.

90. Sahu R, Kaushik S, Clement CC, Cannizzo ES, Scharf B, Follenzi A, et al. Microautophagy of Cytosolic Proteins by Late Endosomes. Dev Cell [Internet]. Elsevier; 2011;20(1):131–9. Available from: http://dx.doi.org/10.1016/j.devcel.2010.12.003.

91. Murrow L, Debnath J. Autophagy as a Stress-Response and Quality-Control Mechanism: Implications for Cell Injury and Human Disease. Annu Rev Pathol Mech Dis. 2012;8(1):121016121742000.

92. El-lakkani A, Elgawad WHA, Sayed EA. Selection of highly efficient small interference RNA (SiRNA) targeting mammalian genes. J Biophys Chem [Internet]. 2013;4(2):72–9. Available from: http://www.scirp.org/journal/PaperInformation.aspx?PaperID=31772&#abstract.

93. Khvorova A, Reynolds A, Jayasena SD. Functional siRNAs and miRNAs exhibit strand bias. Cell. 2003;115(2):209–16.

94. Erfle H, Simpson JC, Bastiaens PIH, Pepperkok R. siRNA cell arrays for high-content screening microscopy. Biotechniques. 2004;37(3):454–62.

95. Dorsett Y, Tuschl T. siRNAs: applications in functional genomics and potential as therapeutics. Nat Rev Drug Discov. 2004;3(4):318–29.

96. Shen D, Coleman J, Chan E, Nicholson TP, Dai L, Sheppard PW, et al. Novel Cell- and Tissue-Based Assays for Detecting Misfolded and Aggregated Protein Accumulation Within Aggresomes and Inclusion Bodies. Cell Biochem Biophys. 2011;60(3):173–85.

97. Gregoire S, Irwin J, Kwon I. Techinques for Monitoring Protein Misfolding and Agregation in Vitro and in Living Cells. Nanostructures, Segmented Polym Compos. 2008;(9):2166–71.

98. Hashimoto T, Adams KW, Fan Z, McLean PJ, Hyman BT. Characterization of oligomer formation of amyloid-beta peptide using a split-luciferase complementation assay. J Biol Chem. 2011;286(31):27081–91.

99. Fuentealba RA, Marasa J, Diamond MI, Piwnica-Worms D, Weihl CC. An aggregation sensing reporter identifies leflunomide and teriflunomide as polyglutamine aggregate inhibitors. Hum Mol Genet. 2012;21(3):664–80.

100. Cox D, Ecroyd H. The small heat shock proteins alfaB-crystallin (HSPB5) and Hsp27 (HSPB1) inhibit the intracellular aggregation of alfa-synuclein. Cell Stress Chaperones. Cell Stress and Chaperones; 2017;27:1–12.

101. Charmpilas N, Kyriakakis E, Tavernarakis N. Small heat shock proteins in ageing and age-related diseases. Cell Stress Chaperones [Internet]. Cell Stress and Chaperones; 2017;1–12. Available from: http://dx.doi.org/10.1007/s12192-016-0761-x.

102. Matsumoto T, Urushido M, Ide H, Ishihara M, Hamada-Ode K, Shimamura Y, et al. Small heat shock protein beta-1 (HSPB1) is upregulated and regulates autophagy and apoptosis of renal tubular cells in acute kidney injury. PLoS One. 2015;10(5):1–22.

103. Picard M, Shirihai OS, Gentil BJ, Burelle Y. Mitochondrial morphology transitions and functions: implications for retrograde signaling? AJP Regul Integr Comp Physiol [Internet]. 2013;304(6):R393–406. Available from:

http://ajpregu.physiology.org/cgi/doi/10.1152/ajpregu.00584.2012.

104. Burté F, Carelli V, Chinnery PF, Yu-Wai-Man P. Disturbed mitochondrial dynamics and neurodegenerative disorders. Nat Rev Neurol [Internet]. Nature Publishing Group; 2014;11(1):11–24. Available from: http://www.nature.com/doifinder/10.1038/nrneurol.2014.228.

105. Reverendo M, Soares AR, Pereira PM, Carreto L, Ferreira V, Gatti E, et al. TRNA mutations that affect decoding fi delity deregulate development and the proteostasis network in zebra fi sh. 2014;(September):1199–213.

106. Schmidt EK, Clavarino G, Ceppi M, Pierre P. SUnSET, a nonradioactive method to monitor protein synthesis. Nat Methods [Internet]. 2009;6(4):275–7. Available from: http://www.nature.com/doifinder/10.1038/nmeth.1314%5Cnhttp://www.ncbi.nlm.nih.gov/pubmed/19305406.

107. Dubey A, Prajapati KS, Swamy M, Pachauri V. Heat shock proteins: A therapeutic target worth to consider. Vet World. 2015;8(1):46–51.

108. Vidyasagar A, Wilson NA, Djamali A. Heat shock protein 27 (HSP27): biomarker of disease and therapeutic target. Fibrogenesis Tissue Repair [Internet]; 2012;5(1):7. Available from: http://fibrogenesis.biomedcentral.com/articles/10.1186/1755-1536-5-7.

109. Huang Q, Ye J, Huang Q, Chen W, Wang L, Lin W, et al. Heat shock protein 27 is over-expressed in tumor tissues and increased in sera of patients with gastric adenocarcinoma. Clin Chem Lab Med. 2010;48(2):263–9.

110. Awasthi N, Wagner BJ. Upregulation of heat shock protein expression by proteasome inhibition: An antiapoptotic mechanism in the lens. Investig Ophthalmol Vis Sci. 2005;46(6):2082–91.

111. Han Y, Moon H, You B, Park W. The effect of MG132, a proteasome inhibitor on HeLa cells in relation to cell growth, reactive oxygen species and GSH. Oncol Rep. 2009;22:215–21.

112. Gregoire S, Kwon I. A revisited folding reporter for quantitative assay of protein misfolding and aggregation in mammalian cells. Biotechnol J. 2012;7(10):1297–307.

113. Ranjan N, Rodnina M V. tRNA wobble modifications and protein homeostasis. Translation [Internet]. Taylor & Francis; 2016;4(1):e1143076. Available from: http://www.tandfonline.com/doi/full/10.1080/21690731.2016.1143076.

114. Patil A, Chan C, Dyavaiah M, Rooney JP, Dedon P. Translational infidelity-induced protein stress results from a deficiency in Trm9-catalyzed tRNA modifications. RNA Biol [Internet]. 2012;9(7):990–1001. Available from: http://www.tandfonline.com/doi/abs/10.4161/rna.20531.

115. Robberecht W, Philips T. The changing scene of amyotrophic lateral sclerosis. Nat Rev Neurosci [Internet]. 2013;14(4):248–64. Available from: http://www.nature.com/doifinder/10.1038/nrn3430.

116. Bendotti C, Marino M, Cheroni C, Fontana E, Crippa V, Poletti A, et al. Dysfunction of constitutive and inducible ubiquitin-proteasome system in amyotrophic lateral sclerosis: Implication for protein aggregation and immune response. Prog Neurobiol [Internet]. Elsevier Ltd; 2012;97(2):101–26. Available from: http://dx.doi.org/10.1016/j.pneurobio.2011.10.001.

117. Fernández-Vázquez J, Vargas-Pérez I, Sansó M, Buhne K, Carmona M, Paulo E, et al. Modification of tRNALysUUU by Elongator Is Essential for Efficient Translation of Stress mRNAs. PLoS Genet. 2013;9(7).

118. Laguesse S, Creppe C, Nedialkova DD, Prévot PP, Borgs L, Huysseune S, et al. A Dynamic Unfolded Protein Response Contributes to the Control of Cortical Neurogenesis. Dev Cell. 2015;35(5):553–67.

119. Tanaka K, Matsuda N. Proteostasis and neurodegeneration: The roles of proteasomal degradation and autophagy. Biochim Biophys Acta - Mol Cell Res [Internet]. Elsevier B.V.; 2014;1843(1):197–204. Available from: http://dx.doi.org/10.1016/j.bbamcr.2013.03.012.

120. Castano M, Akiyama H. Impairment of the Ubiquitin-Proteasome System by Protein Aggregation. Science. 2001;292(May).

121. Urushitani M, Kurisu J, Tsukita K, Takahashi R. Proteasomal inhibition by misfolded mutant superoxide dismutase 1 induces selective motor neuron death in familial amyotrophic lateral sclerosis. J Neurochem. 2002;83(5):1030–42.

122. Verhoef LGGC, Lindsten K, Masucci MG, Dantuma NP. Aggregate formation inhibits proteasomal degradation of polyglutamine proteins. Hum Mol Genet [Internet]. 2002;11(22):2689–700. Available from: http://www.hmg.oupjournals.org/cgi/doi/10.1093/hmg/11.22.2689.

123. Lobanova ES, Finkelstein S, Skiba NP, Arshavsky VY. Proteasome overload is a common stress factor in multiple forms of inherited retinal degeneration. Proc Natl Acad Sci [Internet]. 2013;110(24):9986–91. Available from: http://www.pnas.org/cgi/doi/10.1073/pnas.1305521110.

124. McKinnon C, Goold R, Andre R, Devoy A, Ortega Z, Moonga J, et al. Prion-mediated neurodegeneration is associated with early impairment of the ubiquitin-proteasome system. Acta Neuropathol. Springer Berlin Heidelberg; 2016;131(3):411–25.

125. Songe-Moller L, van den Born E, Leihne V, Vagbo CB, Kristoffersen T, Krokan HE, et al. Mammalian ALKBH8 Possesses tRNA Methyltransferase Activity Required for the Biogenesis of Multiple Wobble Uridine Modifications Implicated in Translational Decoding. Mol Cell Biol [Internet]. 2010;30(7):1814–27. Available from: http://mcb.asm.org/cgi/doi/10.1128/MCB.01602-09.

126. Ohshio I, Kawakami R, Tsukada Y, Nakajima K, Kitae K, Shimanoe T, et al. ALKBH8 promotes bladder cancer growth and progression through regulating the expression of survivin. Biochem Biophys Res Commun [Internet]. Elsevier Ltd; 2016;477(3):413–8. Available from: http://dx.doi.org/10.1016/j.bbrc.2016.06.084.

127. Tang C, Lu Y-H, Xie J-H, Wang F, Zou J-N, Yang J-S, et al. Downregulation of survivin and activation of caspase-3 through the PI3K/Akt pathway in ursolic acid-induced HepG2 cell apoptosis. Anticancer Drugs [Internet]. 2009;20(4):249–58. Available from: http://content.wkhealth.com/linkback/openurl?sid=WKPTLP:landingpage&an=00001813-200904000-00004.

128. Tamm I, Wang Y, Sausville E, Scudiero DA, Vigna N, Oltersdorf T, et al. IAP-family protein Survivin inhibits caspase activity and apoptosis induced by Fas (CD95), bax, caspases, and anticancer drugs. Cancer Res. 1998;58(23):5315–20.

129. Gülow K, Bienert D, Haas IG. BiP is feed-back regulated by control of protein translation efficiency. J Cell Sci [Internet]. 2002;115(Pt 11):2443–52. Available from: http://www.ncbi.nlm.nih.gov/pubmed/12006628.

130. Roy H, Ibba M. Sticky end in protein synthesis. Pharmacogenomics [Internet]. 2013;14(11):1247–50. Available from: http://www.ncbi.nlm.nih.gov/pubmed/23930671.

131. Tamura K. Origins and Early Evolution of the tRNA Molecule. Life (Basel, Switzerland) [Internet]. 2015;5(4):1687–99. Available from: http://www.pubmedcentral.nih.gov/articlerender.fcgi?artid=4695843&tool=pmcentrez&rendertype=abstract.

132. El Yacoubi B, Bailly M, de Crécy-Lagard V. Biosynthesis and Function of Posttranscriptional Modifications of Transfer RNAs. Annu Rev Genet. 2011;46(1):120820103026000.

133. Meiners S, Ballweg K. Proteostasis in pediatric pulmonary pathology. Mol Cell Pediatr [Internet]. 2014;1(1):11. Available from: http://www.pubmedcentral.nih.gov/articlerender.fcgi?artid=4530569&tool=pmcentrez&rendertype=abstract.

Annexes

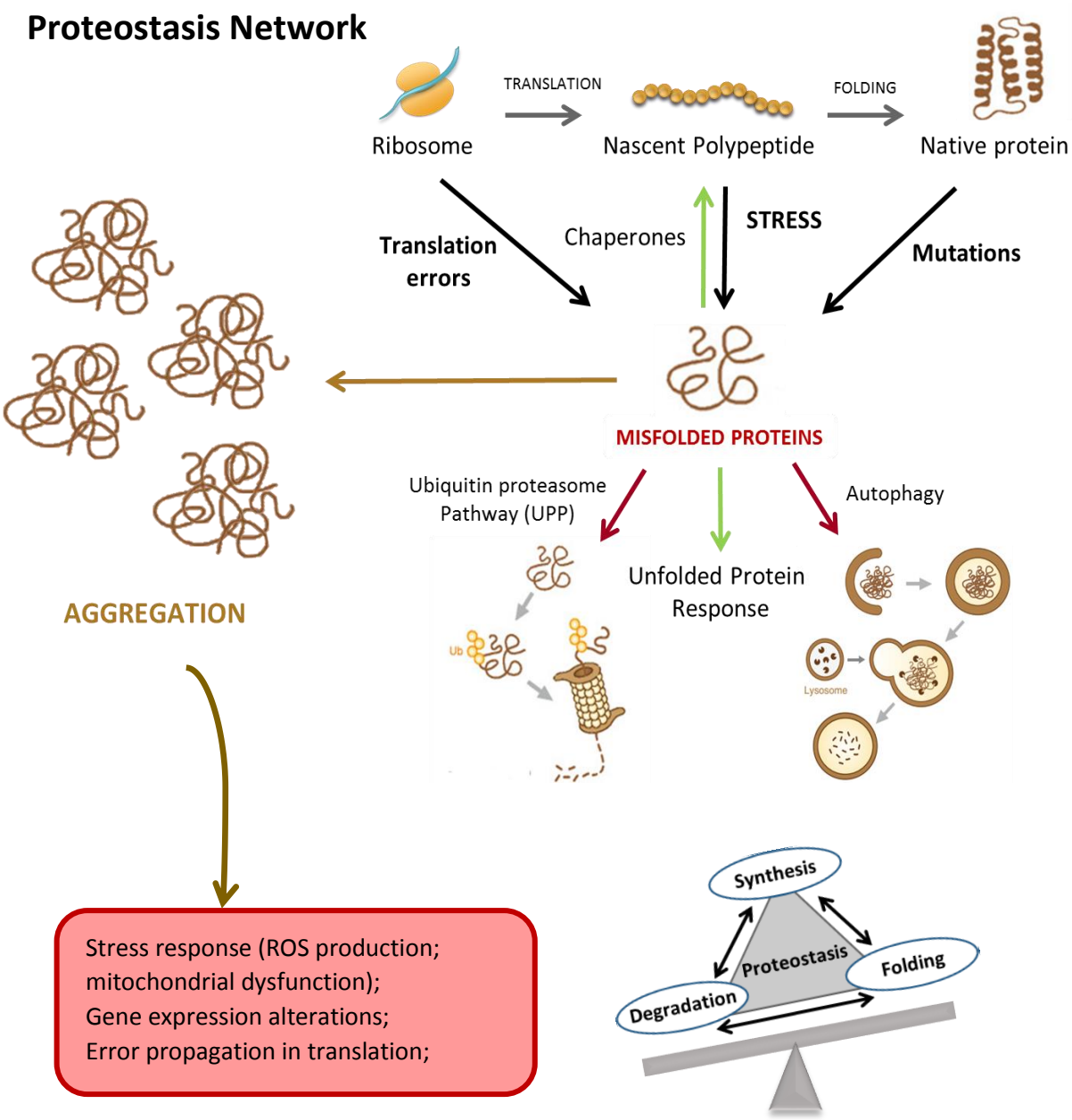

Figure 25: Proteostasis Network. Misfolded proteins in the cytosol or in cellular compartments, such as ER and mitochondria, are recognized by chaperones which support their refolding into the native structure. If misfolded proteins cannot be properly refolded, they are targeted for degradation mainly by the ubiquitin-proteasome system into small peptides. Aggregated protein are surrounded by the autophagosome and degraded after fusion of lysosomes with the autophagosome. Degradation products of the proteasome and the autophagy pathway are mainly recycled as amino acids for protein synthesis. Failure to refold or degrade misfolded proteins can lead to their accumulation and aggregation that interfere with normal protein homoeostasis and resulting in proteotoxic effects. Adapted from: (133).

Table 8: Some human diseases associated with tRNA modifications. Adapted from: (44).

tRNA Modification Related Human Diseases	Modification	Gene involved
Neurological intellectual disability	2´O-methylribose	FTSJ1b
	m_2^2G	TRM1
	m^5C	NSUN2
	m^7G	WDR4c
	A-to-I editing	ADAT3
Familial dysautonomia	mcm^5s^2U	IKBKAP
ALS	mcm^5s^2U	ELP3
Rolandic epilepsy	mcm^5s^2U	ELP4
Dubowitz-like syndrome	m^5C	NSUN2
Cardiac Noonan-like syndrome	m^5C	NSUN2
Respiratory bronchial asthma	mcm^5s^2U	IKBKAP
Cancer skin, breast, and colorectal	m^5C	NSUN2
Breast cancer	wybutosine	TRMT12
Colorectal cancer	m^1G	HRG9MTD2e
Urothelial cancer	mcm^5U	HABH8 (HALKBH8)
Breast, bladder, colorectal, cervix, testicular cancer	mcm^5U	HTRM9L
Epigenetic cancer	m^5C	DNMT2
Metabolic Type 2 diabetes	ms^2t^6A	CDKAL1
MELAS	τm^5U	mt-tRNA Leu (UAA)
MERRF	τm^5s^2U	mt-tRNA Lys (UUU)
Infantile liver failure	S^2U	MTU1 (TRMU)

Abbreviations: mt, mitochondrial; m_2^2G, N2,N2-dimethyl guanosine; m^5C, 5-methylcytosine; m^7G, 7-methylguanosine; mcm^5s^2U, 5-methoxycarbonylmethyl-2- thiouridine; m^5U, 5-methyl uridine; m^1G, 1-methylguanosine; mcm^5U, 5-methoxycarbonylmethyluridine; ms^2t^6A, 2-methylthio-N6-threonyl carbamoyladenosine; tm^5U, 5-taurinomethyluridine; tm^5s^2U, 5-taurinomethyl-2-thiouridine; s^2U, 2-thiouridine.

Table 9: tRNA modifying enzymes selection.

Human tRNA modifying enzyme	Modification
ADAT3	A-to-I editing
IKBKAP	mcm^5U_{34}, $mcm^5s^2U_{34}$, ncm^5U_{34}, ncm^5Um_{34}
Elp2	mcm^5U_{34}, $mcm^5s^2U_{34}$, ncm^5U_{34}, ncm^5Um_{34}
ELP3	mcm^5U_{34}, $mcm^5s^2U_{34}$, ncm^5U_{34}, ncm^5Um_{34}
Elp4	mcm^5U_{34}, $mcm^5s^2U_{34}$, ncm^5U_{34}, ncm^5Um_{34}
Elp5	mcm^5U_{34}, $mcm^5s^2U_{34}$, ncm^5U_{34}, ncm^5Um_{34}
Elp6	mcm^5U_{34}, $mcm^5s^2U_{34}$, ncm^5U_{34}, ncm^5Um_{34}
KTI12	mcm^5U_{34}, $mcm^5s^2U_{34}$, ncm^5U_{34}, ncm^5Um_{34}
TRIT1 (MOD5)	A-to-I editing
URM1	$mcm^5s^2U_{34}$
CTU2	$mcm^5s^2U_{34}$
CTU1	$mcm^5s^2U_{34}$
PUS1	Ψ_{26}, Ψ_{27}, Ψ_{28}, Ψ_{34}, $\Psi_{(35)}$, Ψ_{36}, Ψ_{65}, Ψ_{67}
PUS3	Ψ_{38}, Ψ_{39}
TRMT1	$m^{2,2}G_{26}$
TRMT2A	m^5U_{54}
TRMT2B	m^5U_{54}
NSUN2	m^5C_{34}, m^5C_{40}, m^5C_{48}, m^5C_{49}
ALKBH8 (TRM9)	mcm^5U_{34}, $mcm^5s^2U_{34}$
TRMT10A	m^1G_9
TRMT11	m_2G_{10}
TYW1	yW_{37}
TRMT12	yW_{37}
LCMT2	yW_{37}
TRMU	tRNA-specific 2-thiouridylase (2-thiolation of the wobble base of mt tRNAs)
TRMT5	m1G37, m1I37, yW37
FTSJ1	Cm_{32}, Cm_{34}, $Gm_{34,}$ ncm^5Um_{34}
TRMT61A	m^1A
Qtrt1	Q_{34}
TRDMT1	m^5C_{34}

I. Solutions

Protein Lysis Buffer for Western Blot:

ELB (10 mL)

- Triton X ---------- 50 µL
- Hepes pH=7 (1M) -------- 500 µL
- NaCl (5M) ---------- 500 µL
- H_2O ---------- 8,95 mL

ELB complete (5 mL)

- ELB ---------- 4,645 mL
- *Roche 50x (1 tablet in 2 ml)----- 100 µL
- DTT (1M) ---------- 5 µL
- Naf (1M) ---------- 5 µL
- EDTA (0,5 M) ---------- 20 µL
- EGTA (100 µM) ---------- 50 µL
- *PMSF (40 µM) ---------- 125 µL
- Na_3VO_4 (100 mM) ---------- 50 µL

* Are only added when the use of the ELB!

In addiction: ELB complete (1 mL)

- ELB ---------- 955 µL
- Roche 50x -------- 20 µL
- PMSF ---------- 25 µL

PBS (1L)

Reagents	**Quantities**
NaCl (137 mM)	8,00 g
KCl (2,7 mM)	0,20 g
Na_2HPO_4 (10 mM)	1,44 g
KH_2PO_4 (1,8 mM)	0,24 g

Add H_2O to 1 L and adjust pH = 7.4

Two Acrylamide gels (10%)

Reagents	Resolving (10%) lower	Stacking (4%) upper
ddH$_2$O	3,6 mL	3,464 mL
Tris-Cl	3,75 mL (pH= 8,8)	1 mL (pH= 6,8)
Acrylamide*29.1	2,5 mL	0,5 mL
SDS 10%	100 µL	50 µL
ADS 10%	100 µL	50 µL
TEMED*	10 µL	10 µL

*Acrylamide is a neurotoxin and should be handled with care. ** Added just before pouring gel.

Note: The stacking gel has a low concentration of acrylamide and the running gel a higher concentration capable of retarding the movement of the proteins.

Running Buffer (10x) for SDS-PAGE

Reagents	Quantities
Tris	30,2 g
Glycine	144 g
SDS	10,0 g

Dissolve in 1L of H$_2$0

TBS 10x

Reagents	Quantities
Tris	30,0 g
NaCl	80,0 g
KCl	2,00 g

Add 1L of H$_2$0 and adjust pH = 7.6

Trans-Blot Turbo, Transfer Buffer (1x)

Reagents	Volumes
Tranfer Buffer- 5x	200 mL
Ethanol (~85 %)	200 mL

Add 600 mL of H$_2$0.

Tris-Acetate-EDTA (TAE) Buffer (50x)

Reagents	Concentration
Tris	40,0 mM
EDTA	2,00 mM
Acetic Acid	20,0 mM

Adjust pH = 8.5 and dilute in H_20

"There will come a time when you believe everything is finished.
***That will be the beginning**."*